Wilhoit, R. C., and B. J. Zwolinski, "Physical and Thermodynamic Properties of Aliphatic Alcohols," *J. Phys. Chem. Ref. Data*, 2, Supplement 1 (1973).
Zubarev, V. N., P. G. Prusakov, and L. V. Sergeeva, "Density of Methanol at Atmospheric Pressures," *Zh. Prikl. Khim.*, 47, 1443 (1974).

Manuscript received August 29, 1977; revision received April 20, and accepted June 8, 1978.

A Model For Moving-Bed Coal Gasification Reactors

A steady state model of moving-bed coal gasification reactors has been developed. Model predictions are in agreement with published commercial plant data for Lurgi pressurized gasification reactors and a pilot plant slagging gasifier. The dependence of reactor performance on operating variables has been studied for Illinois and Wyoming coals. For a given coal, maximum efficiency is determined by the coal-to-oxygen feed ratio. The location of the maximum temperature, which defines the combustion zone, is an important operating variable. Efficient operation of the dry ash reactor cannot be carried out below a critical feed gas temperature because of insufficient gasification and excessive carbon loss in the ash.

HEEYOUNG YOON
JAMES WEI
and
MORTON M. DENN
Department of Chemical Engineering
University of Delaware
Newark, Delaware 19711

SCOPE

Moving-bed coal gasification reactors are countercurrent devices in which a coal bed moves downward by gravity flow through an upward flowing gas stream. Steam and oxygen (or air) are fed at the bottom to provide the reactants for the combustion and gasification reactions. The pressurized Lurgi gasifier is commercially proven, while other moving-bed gasifiers, including a potentially high throughput and high temperature reactor that produces a liquid slag, are under development.

The composition and temperature of the product gas and the amount of unburned carbon in the ash largely determine the thermal efficiency of the process. The maximum temperature in the reactor determines the physical state of the ash (dry powder, clinker, slag) and hence the operability of a given reactor configuration. Composition and temperature depend on the properties of the coal being processed and on such operating parameters as feed rates, feed temperature, and reactor pressure. The throughput is limited by the maximum flow rate of steam and oxygen that does not cause entrainment and excessive pressure drop. The performance characteristics of moving-bed gasifiers do not seem to have been studied previously for wide ranges of coal properties, reactor configurations, and operating variables.

We describe here a steady state simulation of a moving-bed gasifier. The model describes the complex physical and chemical processes taking place in the multiphase moving bed, using mass and energy balances and information about rates of chemical reaction and physical transport processes. The use of such a model, following validation with plant data, enables the exploration and prediction of feasible and economically attractive ranges of design and operation in terms of the properties of the coal to be gasified.

CONCLUSIONS AND SIGNIFICANCE

The model has been compared to available commercial plant data for Lurgi reactors and to pilot plant experiments for a slagging reactor. Agreement with experiment is good, and the model has been used to predict the performance of moving-bed reactors for gasification of low activity Illinois and high activity Wyoming coals.

The maximum temperature in the bed is determined largely by the steam-to-oxygen ratio in the feed, while the efficiency at a given steam-to-oxygen ratio is determined by the carbon-to-oxygen feed ratio. In a dry ash reactor, the maximum temperature is limited by the ash fusion temperature, which requires a minimum steam-to-oxygen ratio of approximately seven. In a slagging reactor, the maximum temperature may be much higher, and the steam-to-oxygen ratio may be approximately one. The location of the maximum temperature, which defines the combustion zone, is an important operating variable. If the combustion zone is too low in the Lurgi reactor, then there will be insufficient combustion and an excess of unreacted carbon in the ash. If the zone is too high, there may be too much combustion coupled with insufficient

Heeyoung Yoon is with Conoco Coal Development Company, Libraryville, Pennsylvania 15129. James Wei is with the Department of Chemical Engineering, Massachusetts Institute of Technology, Cambridge, Massachusetts 02139.

0001-1541-78-1610-0885-$02.05.

gasification. The maximum in thermal efficiency occurs at the greatest slope of the curve of height of combustion zone vs. oxygen/carbon feed ratio, suggesting a possible sensitivity in controllability under these operating conditions.

There is a critical blast (steam and oxygen feed) temperature, dependent on the reactivity of the coal, below which efficient operation of the Lurgi reactor cannot be carried out because of excessive carbon loss in the ash and insufficient extent of gasification.

An increased demand of fuel gas can be met by increasing feed rates of coal and gaseous reactants, but relatively more oxygen is required and gasification efficiency is lowered as throughput is increased.

The dry ash and slagging reactors use similar coal-to-oxygen ratios but very different steam-to-oxygen ratios. Much less total gas is needed per unit weight of coal in the slagger, which can therefore accept a four to fivefold increase in coal throughput and gasifier productivity relative to the dry ash reactor.

The overall performance of the slagging reactor is not dependent on coal reactivity, though the position and magnitude of the maximum temperature do depend on reactivity. At carbon-to-oxygen feed ratios below a critical value that is close to the optimum ratio, it may be necessary to operate the slagging reactor with a thin coal bed in order to keep the combustion zone sufficiently close to the bottom of the reactor to allow the slag to run freely without resolidification.

Coal gasification reactors are contacting devices in which coal reacts with air-steam or oxygen-steam gas mixtures. The reactors are designed to convert as large a fraction of the coal as possible to combustible gases, for direct use in power generation, for chemical feedstock, or for upgrading to substitute natural gas.

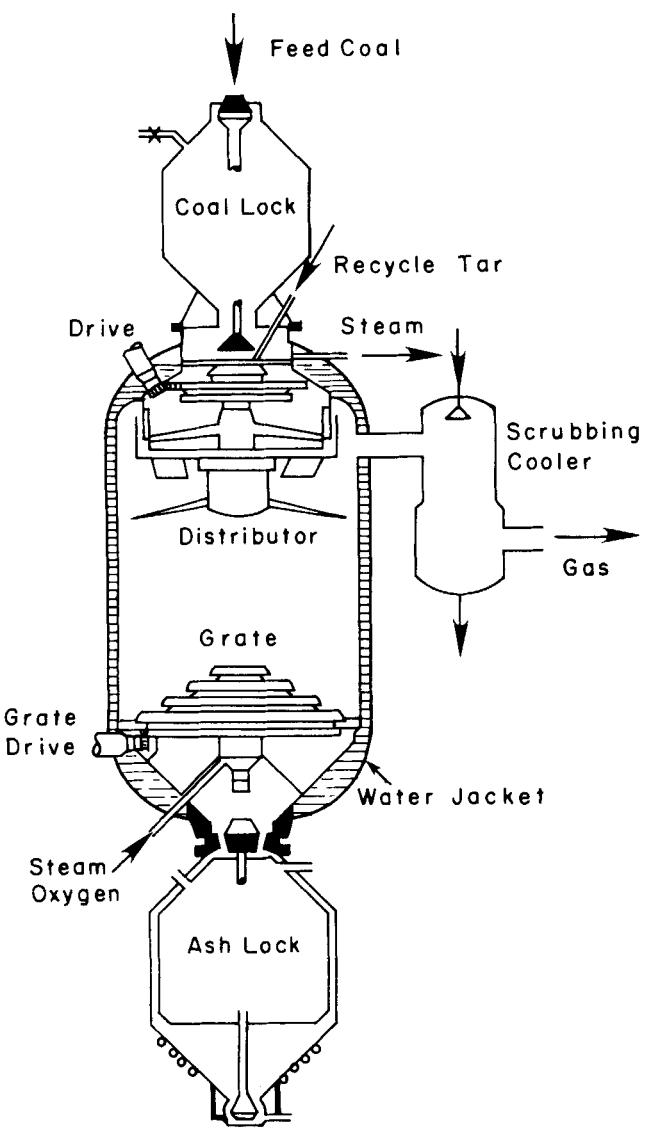

Fig. 1. Lurgi pressurized gasifier.

Gasification reactors can be classified according to the method of contacting between the gas and solid. The most common commercial processes are the Lurgi moving-bed pressurized reactor and the Koppers-Totzek entrained atmospheric reactor. The first Lurgi reactor was put into operation in Hirschfelde, Germany, in 1936, and the first Koppers-Totzek reactor went into operation in Oulu, Finland, in 1952. Other moving bed and entrained configurations are under development, as well as fluidized bed and molten bath reactors.

In the direct contact moving-bed process, coal is fed at the top of the reactor and moves downward by gravity flow, countercurrent to the upward gas flow. Steam and oxygen are fed at the bottom to provide the reactants for combustion and gasification reactions. The Lurgi gasifier is shown in Figure 1. The moving grate at the bottom acts as a gas distributer and removes dry powdered ash. This ash removal system necessitates operation at temperatures below those at which ash clinkers are formed. A slagging reactor (Lacey, 1967; Hebden et al., 1964; Ellman and Johnson, 1976) operates at higher temperatures, and the ash is removed as a liquid slag. The GEGAS reactor (Woodmansee and Floess, 1975; Woodmansee and Palmer, 1977), which has no water jacket, is equipped with a bottom stirrer that can break up clinkers and can operate at higher temperatures than the Lurgi for a given coal. In some moving-bed processes, the tar which is removed from the product gas is recycled to the top of the reactor with the coal feed (Hamm, 1973).

There are several advantages to a pressurized moving-bed process when compared to fluidized and entrained bed processes. The moving bed has a relatively low pressure drop, high thermal efficiency, high carbon conversion, and low entrainment of solids in the gas. Because of the countercurrent flow, the rich gas produced during devolatilization directly enhances the heating value of the product. The primary disadvantage of the moving-bed reactor is the difficulty in processing highly caking coals without pretreatment, though the GEGAS reactor is reported to have been used successfully to gasify a highly caking Pittsburgh coal. A moving bed with diameter greater than 12 ft has not been demonstrated commercially, while fluid beds with diameters greater than 30 ft are commonplace in other applications.

The Lurgi reactor is being planned for use in a combined cycle power process, since the integrated system improves thermal efficiency, reduces investment cost, and meets pollution standards (Krieb, 1973). The individual

units in the combined cycle process are closely coupled, and the performance of the overall system depends critically on the characteristics of each unit. The performance characteristics of moving-bed gasifiers do not seem to have been studied for wide ranges of coal properties, reactor configuration, and feed compositions and rates. Experimental studies have of necessity been limited to narrow ranges of design and operating variables, and available analyses are based largely on untenable equilibrium assumptions (Gumz, 1950). Woodmansee (1976) describes application of the Gumz model and an early rate model by Walker et al. (1937); a more recent model has been published by Klose and Toufar (1976).

We describe here the development of a steady state simulation model for a moving-bed gasifier. The model is compared to available plant data for Lurgi reactors and to pilot plant experiments for a slagging reactor; it is used to predict the performance of moving-bed reactors for gasification of low activity Illinois and high activity Wyoming coals. The model describes the complex physical and chemical processes taking place in the multiphase moving bed by use of mass and energy balances, together with information about rates of chemical reaction and physical transport processes. The use of the model, following validation with plant data, enables the prediction of feasible and economically attractive ranges of design and operation in terms of the properties of the coal to be gasified.

DEVELOPMENT OF THE MODEL

Description of Moving-Bed Gasifier

In a moving-bed gasification reactor, the solid phase, coal, moves downward under gravity flow countercurrent to the upward flowing gas stream. The Lurgi moving-bed gasifier is shown schematically in Figure 1. This reactor is pressurized, and coal is fed to the top through a pressurized lock hopper. Steam and oxygen are fed to the bottom. The reactor can be run with air instead of oxygen, and air operation is planned for the Powerton combined cycle power process test facility in Illinois.

During steady state operation, coal descends through regions of increasing temperature and solid disintegration. It is helpful conceptually, following Krieb (1973), to think tentatively of zones in the reactor of distinct physical and chemical processes. The first zone in this idealization is one in which the coal is preheated and dried through heat exchange between the coal and the hot gas. This is followed by a devolatilization zone, in which coal gases and tars are expelled. The third zone in the descent is gasification, where carbon monoxide and hydrogen are mainly formed by steam-carbon reduction. There is no oxygen in the gas in this zone. The final zone is one of combustion and ashing. In reality, some or all of these zones will overlap. Moe (1973), for example, combines gasification and devolatilization into a single zone. As we shall see from the results reported here, for some coals there may be no clear demarcation between the combustion and gasification zones. The exothermic combustion reaction provides the energy needed for the endothermic processes such as gasification and drying.

As shown in Figure 1, there is a water jacket on the wall of the Lurgi gasifier, and part of the process steam is produced in the jacket by the heat transferred from the coal bed. Because of low heat conductivity of the coal bed, most of the reactor cross section is unaffected by the heat loss. However, the heat loss cools down the coal near the wall and has a major effect on the energy balance in this region. The reactor may be thus visualized as consisting of the two different regions shown schematically in Figure 2, the adiabatic core occupying most of the reactor space and the colder boundary layer occupying an annular portion of the coal bed surrounding the adiabatic core. In the model development, it is assumed that the heat loss only affects the boundary layer, and there is no heat flow from the adiabatic core to the boundary layer. The thickness of the boundary layer is estimated subsequently from the properties of the coal, the wall and jacket, and the operating conditions of the gasifier. It is assumed that the gases leaving the adiabatic core and the boundary layer are completely mixed at the top of the reactor.

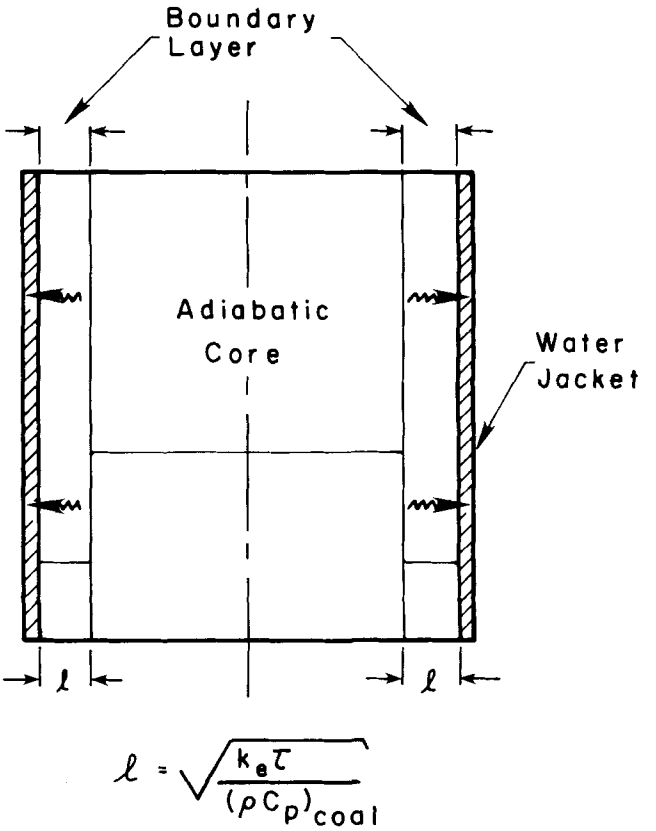

Fig. 2. Schematic of adiabatic core and boundary layer.

If the reactor has a refractory wall, as in the GEGAS pressurized gas producer, the heat loss through the reactor wall may be sufficiently small that the boundary layer need not be considered in modeling the reactor.

Combustion and Gasification

The dominant processes in the lower portion of the reactor are heterogeneous reactions between carbon and components of the gas stream. The following reactions are assumed to occur between solid carbon and gaseous reactants:

Gasification:

$$C + H_2O \rightleftarrows CO + H_2 \quad (1)$$

$$C + CO_2 \rightleftarrows 2CO \quad (2)$$

$$C + 2H_2 \rightleftarrows CH_4 \quad (3)$$

Combustion:

$$\lambda C + O_2 \rightarrow 2(\lambda - 1)CO + (2 - \lambda)CO_2 \quad (4)$$

The three gasification reactions are all reversible. λ is a system constant, dependent on reaction conditions, which determines the primary product distribution of carbon monoxide and carbon dioxide in the combustion products.

Table 1. Equilibrium Parameters

Reaction	K°_i	ΔH°_i (cal/mole)	Reference
1. Carbon-steam	3.098×10^7	32 457	Hottel and Howard (1971)
2. Carbon-carbon dioxide	1.222×10^9	40 300	Parent and Katz (1948)
3. Carbon-hydrogen	1.472×10^{-6}	−21 854	Hottel and Howard (1971)
4. Water-gas shift	0.0265	−7 860	Parent and Katz (1948)

The molar ratio of carbon monoxide/carbon dioxide in the combustion reaction follows an Arrhenius temperature relation (Arthur, 1951; Rossberg, 1956), with the parameters (particularly the preexponential factor) dependent on oxygen pressure, carbon burn-off, and surface oxide coverage (Phillips et al., 1969, 1970). Data are not available at the high oxygen pressure characteristic of the moving-bed gasifier, but high pressure favors the formation of carbon dioxide. Because of the uncertainty, λ is taken as a constant despite the variation in temperature and composition in the oxidation zone. The dependence of model behavior on λ is discussed in a later section.

In addition to the four heterogeneous reactions, the water gas shift reaction occurs in the gas phase catalyzed by coal particles:

Water gas shift:

$$CO + H_2O \rightleftarrows CO_2 + H_2 \qquad (5)$$

It is assumed that the water gas shift reaction is in equilibrium at all positions of the reaction zone. An error in this assumption would introduce only a small error in the energy balance because of the slight exothermicity of the reaction, and the gasification rate will not be affected (Ergun and Menster, 1965).

The equilibrium constants for reactions (1), (2), (3), and (5) follow an Arrhenius temperature dependence

$$K_i = K_j^\circ \exp\left(-\Delta H_i^\circ / RT\right) \qquad (6)$$

The equilibrium parameters are recorded in Table 1.

Gas phase combustion of hydrogen and carbon monoxide may occur, but it is not clear to what extent these homogeneous reactions can take place during the short residence time of the combustion zone. The recent calculation by Edgar et al. (1976) implies that the extent of these reactions will not be significant in a packed-bed coal reactor, and they are not considered here. The validity of neglecting gas phase oxidation will be discussed later by comparing the model predictions to actual plant data.

We assume that there are no important radial gradients in either the adiabatic core or the boundary layer. This assumption results in discontinuities of temperature and concentrations at the boundary of the two regions. The mass balances for fixed carbon, oxygen, steam, and methane can be written, respectively, in both the adiabatic core and the boundary layer as follows:

Carbon:

$$F^\circ_C \frac{dw}{dz} = r_1 + r_2 + r_3 + \lambda r_4 \qquad (7)$$

Oxygen:

$$F^\circ_{O_2} \frac{dx}{dz} = r_4 \qquad (8)$$

Water:

$$F^\circ_{H_2O} \frac{dy}{dz} = r_1 \qquad (9)$$

Methane:

$$F^\circ_{H_2O} \frac{dv}{dz} = r_3 \qquad (10)$$

Here z is the distance from the bottom of the reaction zone; w is the fraction of unreacted fixed carbon; x and y are the fractional conversions of oxygen and steam, respectively; and v is the dimensionless amount of methane in the gas stream relative to inlet steam feed flux.

The functions r_1, r_2, r_3, and r_4 are the apparent rates of the corresponding chemical reactions given by Equations (1) through (4) and depend on the local composition of the gas phase and the concentration of fixed carbon as well as the local temperature. f_i is the molar feed flux of component i.

With the further assumption that solid and gas temperatures are the same, and neglecting the heat loss from the adiabatic core to the adjacent boundary layer, the energy equation for the adiabatic core is

$$(H_S - H_G)\frac{dT}{dz} = r_1\Delta H_1 + r_2\Delta H_2 + r_3\Delta H_3 + r_4\Delta H_4 \qquad (11)$$

For the boundary layer, the inclusion of the heat loss through the wall leads to the following energy equation:

$$(H_S - H_G)\frac{dT}{dz} = r_1\Delta H_1 + r_2\Delta H_2 + r_3\Delta H_3 + r_4\Delta H_4 + hA(T - T_w) \qquad (12)$$

H_S and H_G are the heat capacity fluxes (heat capacity at constant pressure per unit mass multiplied by mass or mole flux) of solid and gas phases, respectively, and ΔH_i are the enthalpies of reactions corresponding to Eqs. (1) through (4). A is an effective wall heat transfer surface area per unit volume of the boundary layer, h is the overall heat transfer coefficient between the coal bed in the boundary layer and the water in the jacket, and T_w is the temperature of water in the jacket.

The overall mass balances for carbon, hydrogen, and oxygen from the bottom of the reactor to position z relate the local fluxes F_i of gaseous components to the variables x, y, v, and w, and the feed conditions. These balances are given in Table 2. The partial pressure P_i of each component can then be expressed in terms of the operating pressure P as

$$P_i = P\,\frac{\text{flux of component } i\ (F_i)}{\text{total gaseous flux } (F_G)} \qquad (13)$$

Table 2. Local Fluxes of the Gas Phase Components

Component (i)	Flux (F_i)
(1) H_2O	$F^\circ_{H_2O}(1 - y)$
(2) CO_2	$F^\circ_{H_2O}[y + 2ax - b(w - w_B) + v]$
(3) H_2	$F^\circ_{H_2O}(y - 2v)$
(4) O_2	$F^\circ_{H_2O}\,a(1 - x)$
(5) CO	$F^\circ_{H_2O}[2b(w - w_B) - y - 2ax - 2v]$
(6) CH_4	$F^\circ_{H_2O}\,v$
Total	$F^\circ_{H_2O}[1 + a - ax + b(w - w_B) - 2v]$

a: oxygen to steam molar feed ratio
b: fixed carbon to steam molar feed ratio
w_B: fraction of fixed carbon remaining in the ash

H_G depends on the local fluxes of gaseous components as follows:

$$H_G = \sum_i F_i C_{pi} \tag{14}$$

Here, C_{pi} is the molar heat capacity of component i in the gas. The solids heat capacity flux H_s is

$$H_s = F^\circ_C \, w \, C_{pc} + G^\circ_{\text{coal}} \, f_{\text{ash}} \, C_{p\text{ash}} \tag{15}$$

Here, C_{pc} and $C_{p\text{ash}}$ are the molar and mass heat capacities of carbon and ash, respectively; f_{ash} is the weight fraction of ash as given by the proximate analysis; and G°_{coal} is the mass feed flux of coal.

It is assumed that the heat capacity of ash is the same as that of carbon. This assumption will not create any significant error in modeling for most coals. As z increases, more material passes from the solid to the gas phase, so that the values of both H_G and H_s increase, while the difference remains nearly the same. Since the range of temperatures considered is large, the heat capacities of solid and gaseous components and the heats of reaction are taken to be functions of temperature, using data from Hougen et al. (1954), Kelly and Taylor (1973), and Lavrov (1963).

Axial heat and mass dispersion have been neglected in Equations (7) through (12). Heat transfer in a packed bed can occur by several mechanisms (Yagi and Kunii, 1957). Turbulent mixing and radiation are the dominant mechanisms in the moving-bed gasifier owing to the high axial flux of the gaseous stream and the high temperature. The effect of turbulent mixing on thermal conduction was estimated from the axial Peclet number for mass transfer and that of radiation by following Chen and Churchill (1963). The effective thermal conductivity by these two mechanisms is about 9.52 W/m°K at 1 100°C (5.5 Btu/hr ft °F at 2 000°F) temperature for a 10 mm (0.4 in.) average diameter coal particle at standard Lurgi operation conditions. Heat transfer is mostly due to turbulent mixing, and radiation contributes about 10% of the effective thermal conductivity. The conductivity is estimated at a coal-bed temperature of 1 100°C, since it is believed to be near the maximum temperature in the bed of the Lurgi gasifier, and thus the estimate represents the upper bound. With this effective conductivity, the Peclet number, a measure of the importance of the axial heat conduction, is about 500 for the whole bed and 1.6 for a particle distance. This means that the bed can be approximated by 250 stirred-tank reactors in series (Levenspiel, 1972) and is approximately a piston flow reactor without thermal dispersion. In a typical operation, the residence time of coal is about 1 hr, and the residence time of gas is of the order of 10 s. In the slagging and GEGAS gasifiers, the maximum temperature is higher than that in the Lurgi gasifier, and the thermal conductivity by radiation may be bigger than the above estimate. The Peclet number for these systems should not be less than 50, however, so that the piston flow assumption is still satisfactory. The effect of neglecting the thermal axial diffusion will be discussed further later.

The water-gas shift reaction, Equation (5), is not included in the rate process model given by Equations (7) through (12) because of the assumption of equilibrium at every point in the reactor. From the point of view of digital computer solution this deletion is unimportant, since for each step in numerical integration the physical and chemical processes can be considered as having two steps. The first is rate controlled and is given by Equations (7) through (12). The second is instantaneous and is given by the equilibrium

$$P_{H_2} P_{CO_2} = P_{H_2O} P_{CO} \, K^\circ_5 \exp(-\Delta H^\circ_5 / RT) \tag{16}$$

The correction to the temperature at each step resulting from the equilibrium is then

$$\delta T = -\Delta H_5 F^\circ_{H_2O} \, \delta y / (H_G - H_S) \tag{17}$$

where δy is the adjustment to the steam conversion required by the water-gas shift equilibrium (16). ΔH_5 is given by Lavrov (1963), and the values of ΔH°_5 and K°_5 are given in Table 1. In principle, it is possible to eliminate any one of the Equations (7) to (10) describing the differential mass balances of the system by applying the algebraic relation Equation (16) to them. However, such substitution makes the differential energy balance equation very complex and does not help to simplify the model equations numerically. The equilibrium assumption has been verified by calculations in which water-gas shift kinetics are included in the mass balance equations.

The combustion and gasification reactions take place over a wide temperature range, and at various positions the apparent rate may be controlled by the intrinsic reaction rate or by pore or bulk film diffusion rates. The intrinsic reaction rates are assumed to follow mass action laws, and their coefficients follow the Arrhenius law

$$k_{r,i} = k_{i,o} \exp(-E_i / RT) \tag{18}$$

Values of the kinetic parameters need to be determined from experimental data for the particular coal of interest.

The bulk film mass transfer coefficient is obtained from a j factor correlation given by Gupta and Thodos (1963). For a Reynolds number of order 200, which is a value characteristic of the Lurgi gasifier, the correlation can be rearranged to the form

$$k_{p,i} = \frac{2.06}{\epsilon P} Sc^{-0.092} \, (PD_i / d_p RT)^{0.575} \, F_G^{0.425} \tag{19}$$

Here, d_p is the particle diameter, ϵ is the void fraction of the coal bed, D_i is the bulk phase diffusivity of gas species i, and F_G is the total molar flux of gas.

Equation (19) is also applicable to the slagging and GE gasifiers, since their Reynolds numbers are within the range of the correlation ($90 \leq Re \leq 4\,000$).

We have considered two different physical models of the coal particle behavior during the combustion and gasification reactions, as shown schematically in Figure 3. Figure 3*a* shows the case in which the coal burning takes place by a shell progressive (SP model) mechanism (compare Jensen, 1975), where it is assumed that the ash retains its structure and remains on the coal particle to form an ash layer surrounding an unreacted core. Figure 3*b* shows the case in which it is assumed that the ash remaining following the reactions is segregated (AS model) from the coal particle, and there is no ash layer between the combustible fixed carbon and the gaseous reactants. The true behavior of ash is between these limiting cases in the Lurgi gasifier. If the amount of ash in the coal is small, it may be better represented by the AS model, and the AS model should apply to the slagging gasifier, where the molten slag drips off the coal particles.

We assume that the carbon-oxygen (4) and carbon-steam (1) reactions are limited by intraparticle diffusion rates of oxygen and steam as well as by intrinsic reaction rates. With the SP model, we have for these two reactions of gaseous attack on carbon (Aris and Amundson, 1973)

$$r_i = \frac{(1-\epsilon)(P_i - P_i^*)}{\dfrac{d_p^\circ}{6k_{p,i}} + \dfrac{d_p^{\circ 2}(1-\rho)RT}{12\rho D_{M,i}} + \dfrac{1}{\eta_i \rho^3 k_{r,i} C_c^\circ}} \tag{20}$$

Here, P_i^* is the equilibrium partial pressure of reactant i for oxygen, P_i^* is practically zero d_p° is the initial solid

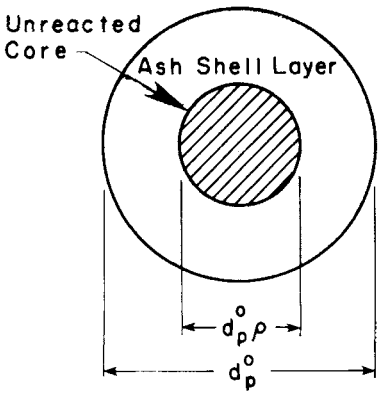

Fig. 3a. Schematic of shell progressive (SP) model.

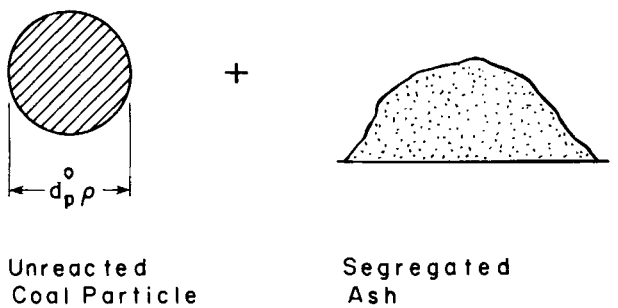

Fig. 3b. Schematic of ash segregation (AS) model.

particle diameter, ρ is the fraction of the particle diameter which is occupied by unreacted core, and C_c° is the initial concentration of fixed carbon in the particle. $k_{r,i}$ is the intrinsic reaction rate coefficient for the reaction i, $k_{p,i}$ the film mass transfer coefficient for the gaseous species in reaction i, $D_{M,i}$ the effective diffusivity of the gaseous species in reaction i in the outer shell of the particle, and η_i is the effectiveness factor for the reaction in the core.

For oxygen, P_i^* is practically zero. For a spherical porous core, η_i is given by the expression

$$\eta_i = \frac{1}{\phi_i}\left(\frac{1}{\tanh(3\phi_i)} - \frac{1}{3\phi_i}\right) \tag{21}$$

The Thiele modulus for reaction i is defined by

$$\phi_i = \frac{d_p^\circ \rho}{6}\sqrt{\frac{k_{r,i} C_c^\circ}{\gamma_i D_{e,i}/RT}} \tag{22}$$

where $D_{e,i}$ is the effective diffusivity of the gaseous species in reaction i in the core of the particle.

$\gamma_i = \lambda$ for the combustion reaction, and $\gamma_i = 1$ for the carbon-steam reaction. The effective diffusivities in the outer shell and also in the core of the particle are estimated by the following formula proposed by Walker et al. (1959):

$$\text{Shell:} \quad D_{M,i} = D_i \theta_s^2 \tag{23}$$

$$\text{Core:} \quad D_{e,i} = D_i \theta_c^2 \tag{24}$$

θ_s and θ_c are void fractions of the particle in the shell and core, respectively.

With the AS model we have

$$r_i = \frac{(1-\epsilon)(P_i - P_i^*)V_c}{\dfrac{d_p^\circ(1-\rho)}{6k_{p,i}} + \dfrac{1}{\eta_i k_{r,i} C_c^\circ}} \tag{25}$$

Here, η_i is also defined by Equation (21), and V_c is the fraction of space occupied by the unreacted coal particle:

$$V_c = \frac{w}{w + \dfrac{(1-w)\rho_{\text{coal}} f_{\text{ash}}}{\rho_{\text{ash}}}} \tag{26}$$

ρ_{coal} and ρ_{ash} are the densities of the original coal and of the ash segregated from the coal particle.

We assume that the carbon-carbon dioxide (2) and carbon-hydrogen (3) reactions are controlled by their intrinsic reaction rates, since hydrogen and carbon dioxide are reaction products formed in the particle and become reactants in the gasification reaction. This assumption could introduce some error near the combustion zone, where the concentrations of hydrogen and carbon dioxide change rapidly.

Possible carbon formation and deposition is allowed for in the model by inclusion of the reverse reactions for gasification by steam and carbon dioxide. These reverse reactions can take place if the reactor is sufficiently cold and are most likely to occur in the boundary layer.

Drying and Devolatilization

The upper zone is a region in which the coal is heated and dried and devolatilized. Heating and drying are rapid and can be considered for modeling purposes to be instantaneous. We have generalized the coal drying analysis used by McIntosh (1976) to include the influence of the flux of water in the solid particle and temperature transients in the undried core. This analysis shows that drying time is proportional to the square of the average particle diameter. The average diameter was obtained by applying the formula proposed by Kunii and Levenspiel (1969) to the data on coal particle distribution given by Lacey (1967). Using parameters typical of conditions in the Lurgi gasifier, we estimated a heating and drying time of the order of 60 to 90 s for coal with a 10% moisture content. This time is small in comparison to a solids residence time of the order of 1 hr or more in the dry ash reactor and 10 to 15 min in the slagger. In the slagging and GEGAS gasifiers, the gas temperature entering the drying zone is much hotter than the temperature in the Lurgi gasifier, and the drying of coal in those gasifiers will be even more rapid.

Anthony and Howard (1976) have recently reviewed the available fundamental information on devolatilization. This phenomenon is still not completely understood. The mechanisms involved in devolatilization depend on such operating conditions as temperature, pressure, particle size, constituents of carrier gas, and the particular coal (Wen et al., 1967; Friedman et al., 1968; Anthony and Howard, 1976) as well as the heating rate (Jünten and Van Heek, 1968). There are even conflicting views as to whether the net process is endothermic or exothermic (Berkowitz, 1957; Gaines and Partington, 1960). Devolatilization in the presence of hydrogen at high pressure is believed to create a "super-active" carbon, which re-

Table 3. Typical Devolatilization Data

Fractional distribution of volatiles (wt %)	
Tar, oil plus phenol	20%
Chemical water	23%
Coal gas	57%
Distribution of coal gas (% v/v)	
CH_4	50.3
H_2	13.1
CO	20.6
CO_2	6.1
Others (hydrocarbons, H_2S, N_2)	9.9

sults in a rapid carbon-hydrogen reaction to form methane (Feldman, 1975; Wen et al., 1967; Anthony and Howard, 1976).

The fractional distribution of devolatilization product also depends on operating conditions. It is believed that cracking of tar occurs in a moving-bed gasifier, since the amount of tar produced from gasifier plant operation has ranged only from 10 to 25% of volatile matter (Elgin and Perks, 1974; Moe, 1973; Hoogendorn, 1973; Woodmansee and Palmer, 1976), while laboratory data on devolatilization typically show more than 50% of the volatile matter produced to be tar (Anthony and Howard, 1976).

No attempt has been made to construct a detailed devolatilization model. It is assumed that the net thermal effect is neutral, and that the portion of the coal to be devolatilized is the same as the portion of volatile matter determined by the proximate analysis. Two different methods are used to estimate the distribution of devolatilization products. The first method simply uses typical devolatilization data as given in Table 3 and does not distinguish between coal types; the coal gas distribution for devolatilization in the moving-bed reactor is assumed to be the same as the distribution given by Loison and Chauvin (1964), despite the difference between the fraction of volatiles appearing as coal gas in the laboratory experiment and in the moving-bed reactor. This method does not require detailed information about the ultimate analysis and devolatilization products of each individual coal, but it will cause some errors in overall mass balances of elements.

The second method requires both the ultimate analysis and laboratory devolatilization data for the coal. It is assumed that 20% of the volatile matter appears as tar and oil plus phenol (0% if the tar is recycled), and the remainder is cracked to the stoichiometric proportions of methane, carbon monoxide, and hydrogen. The tar is assumed to have a chemical formula $C_1H_1O_{0.05}$ (Lacey, 1967; Kimmel et al., 1976). Since there are only three elements in this formula, only three cracking reaction products can be allowed for a deterministic system. (In some cases, the production of hydrogen or carbon monoxide may be negative, in which case they are assumed to be acting as reactants consumed in the cracking of tar.) All of the sulfur in the coal is assumed to appear as hydrogen sulfide during devolatilization, following Elgin and Perks (1974), Kimmel et al. (1976), and Moe (1973).

The particular assumptions made in modeling devolatilization are not critical in determining overall reactor performance, because the gas produced through devolatilization contributes only a small portion of the total gas formed in the reactor (about 10%), and the conditions for devolatilization encountered in the moving-bed gasifier do not change significantly under normal operating conditions.

The kinetics of devolatilization are believed to be first order (Wiser, 1968; Van Krevelen, 1961), so that the mass balance has the form

Table 4. Distribution of Components in Coal by Proximate Analysis (Elgin and Perks, 1974; IGT Report, 1976)

	Illinois coal	Wyoming coal
Moisture	10.23	17.06
Ash	9.10	5.80
Fixed carbon	45.97	43.20
Volatile matter	34.70	33.94

$$\frac{df}{dz} = k_{v,o} \exp(-E_v/RT) \cdot f \qquad (27)$$

f is the fraction of volatile material remaining in the coal particles.

It is known that devolatilization occurs through two successive stages (Van Krevelen, 1961). Primary devolatilization is almost instantaneous, and much of the volatile matter is devolatilized during this stage. The remaining volatile matter is devolatilized through the relatively slow secondary devolatilization, and thus the two stages have different rate parameters E_v and $k_{v,o}$. Even for the same stage, these parameters depend on the properties of coal and operating conditions; these are given in the review paper by Anthony and Howard (1976). The rates are sufficiently fast that they are assumed here to be instantaneous.

Estimation of Boundary-Layer Thickness

We have estimated the thickness of the boundary layer by calculating the Einstein length for the operating conditions of the Lurgi gasifier (Carslaw and Jaeger, 1959):

$$l = \sqrt{\alpha\tau} \qquad (28)$$

where $\alpha = k_e/(\rho C_p)_{coal}$ is the radial thermal diffusivity of the coal bed. k_e is the radial effective thermal conductivity of the bed, and τ is the residence time of coal in the gasifier. k_e was estimated following Argo and Smith (1953) and Chen and Churchill (1963); it has two major contributions, radial turbulent mixing and radiation. The value of k_e is 2.60W/m°K at 1 100°C (1.50 Btu/hr ft°R at 2 000°F), the approximate maximum temperature of the bed. If we assume that the coal bed is uniform at 1 100°C, the thickness is computed from Equation (28) to be about 9.4 mm (3.7 in.) at the bottom of the dry ash reactor. It is taken here to be 9.4 mm. (We also estimated the thickness of the boundary layer in terms of the properties and residence time of the gas phase, assuming that the coal is stationary. The estimated thickness by this method is about the same.) From the reported production rate of steam in the jacket, which is about 10 to 20% of the process steam (Rudolph, 1972; Elgin and Perks, 1974), the overall heat transfer coefficient from the coal bed in the boundary layer to the cooling water in the jacket was estimated to be 307 W/m²°K (54 Btu/hr ft²°R), which would be reasonable for con-

Table 5. Reaction Parameters

Reaction	k_{io}	E_i (cal/mole)	Reference
1. Carbon-steam (Illinois coal)	613 (moles/mole C atm s)	42 000	Gibson and Euker (1975)
(Wyoming coal)	412 (moles/mole C atm s)	35 000	Gibson and Euker (1975)
3. Carbon-hydrogen (Wyoming coal)	8.36×10^{-4} (moles/mole C atm² s)	16 050	Gibson and Euker (1975)
4. (Combustion)	1.79×10^{6} (moles/mole C atm s)	27 000	Sergent and Smith (1973)

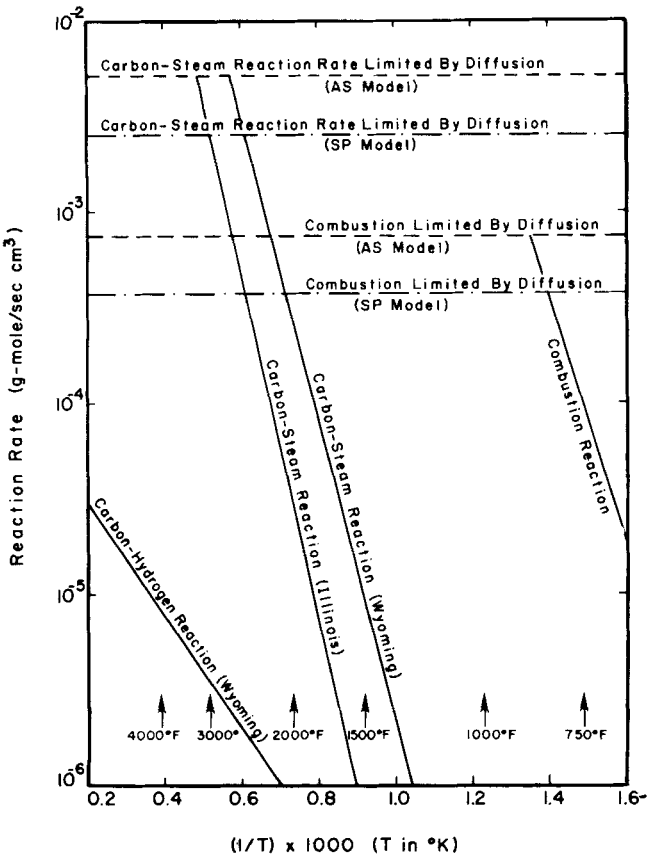

Fig. 4. Reaction rates of combustion and gasification.

vection to an unlined steel wall (Lowry, 1963). For the slagger, temperature and k_e are somewhat higher than in the Lurgi, but the residence time is smaller by a factor of four to five, so the boundary-layer thickness may be only half as large.

Equation (28) shows that the thickness of the boundary layer does not depend on the diameter of the gasifier. As the diameter of the gasifier becomes larger, the contribution of the boundary layer becomes less important. If a gasifier has a thick refractory wall, the overall heat transfer coefficient is so small that the behavior of the boundary layer is not much different from that of the adiabatic core, and thus it may not be necessary to consider the boundary layer separately in predicting the performance of the gasifier. No attempt has been made to estimate the thickness of the boundary layer for the GEGAS gasifier.

APPLICATION TO THE OXYGEN-BLOWN LURGI GASIFIER

The model developed in the previous section has been used to simulate the performance of the oxygen blown Lurgi gasifier. This system was chosen because the existing plant data provide a useful comparison for validation of the model.

Model Predictions

The differential mass and energy balance equations for both the adiabatic core and the boundary layer were solved numerically, subject to the following boundary conditions:

at	$z = 0$	$T = T_b$	bottom of reactor
		$x = 0$	
		$y = 0$	
		$v = 0$	
at	$z = L$	$w = 1$	top of reactor
		$f = 1$	

The equations for T, x, y, v, and w form a fifth-order boundary-value problem and must be solved iteratively to match the boundary conditions; the equation for f is uncoupled. We have used the Runge-Kutta fifth-order method for the integration and the Fibonacci search method for matching boundary conditions. Calculations were done for Illinois and Wyoming coals. The distribution of components in these coals is given in Table 4.

The values of the kinetic parameters for these two coals are given in Table 5. It is assumed that both of these coals have the same combustion reaction rate parameters and the same value of λ equal to 1.333. Following Ergun and Menster (1965), in the absence of more concrete data for reaction (2), we take

$$k_{r,2} = 0.6\, k_{r,1} \tag{29}$$

For the methane formation reaction, there are no data available for Illinois coal. It is assumed that the methane formation intrinsic reaction rate coefficient for Illinois coal is one-tenth of that shown in Table 5 for Wyoming coal, since the steam-carbon reaction rate coefficients of these two coals differ by a factor of ten.

Figure 4 shows the Arrhenius plots of the carbon-oxygen, carbon-steam, and carbon-hydrogen rates, using the kinetic parameters in Table 5. The rates are also shown when the reactions are limited by gas-film and pore diffusion of gaseous reactants for the SP model and by gas-film diffusion for the AS model for a 1 cm diameter particle. The reaction rate limited by the diffusional resistance shown in Figure 4 is higher for the carbon-steam reaction than for the combustion reaction, because the gaseous feed is assumed to have a steam to oxygen feed ratio of 6.8, and thus the partial pressure of steam is 6.8 times that of oxygen. Because the diffusion limitations are significant where the bed temperature is high and the reactions are intense, calculations of the diffusion rates for Figure 4 were done with Equation (19) at 1 100°C (2 000°F) and 50% carbon conversion. These numbers are the probable ones in the intense reaction zone of the gasifier operated at the conditions given in Table 6. For the carbon-steam and combustion reactions, gas compositions were assumed to be the same as the feed conditions, for the estimation of the intrinsic reaction rates as well as the diffusion controlled reaction rates. For the carbon-hydrogen reaction, hydrogen concentration is assumed to be at the value of 50% carbon conversion. The thickness of the gas film at these conditions was estimated from Equation (19) to be about 1.2 mm. For the SP model, the thickness of the ash shell on a 10 mm diameter particle is 1 mm when the conversion is 50%.

Figure 4 shows that the diffusion limited reaction rates are lower for the SP model than for the AS model because of the addition of the pore diffusion resistance in the SP model. As a result of this earlier limitation in the SP model, the maximum temperature predicted by that model is expected to be lower than the maximum temperature by the AS model, since the combustion and gasification reactions are comparable in the SP model at a reduced temperature. (The simulation calculations show this difference for both Illinois and Wyoming coals.)

The height of the coal bed from the grill to the distributor inlet was taken to be 3.05 m (10 ft), and the diameter of the coal bed was taken to be 3.66 m (12 ft).

Adiabatic Core. This region represents the major portion of the gasifier and primarily determines the performance of the entire gasifier. The temperature profile in the core is of particular interest in gaining an understanding of the interactions between the various physicochemical processes. Figures 5*a* and *b* show temperature profiles using the SP and the AS models, respectively, for both

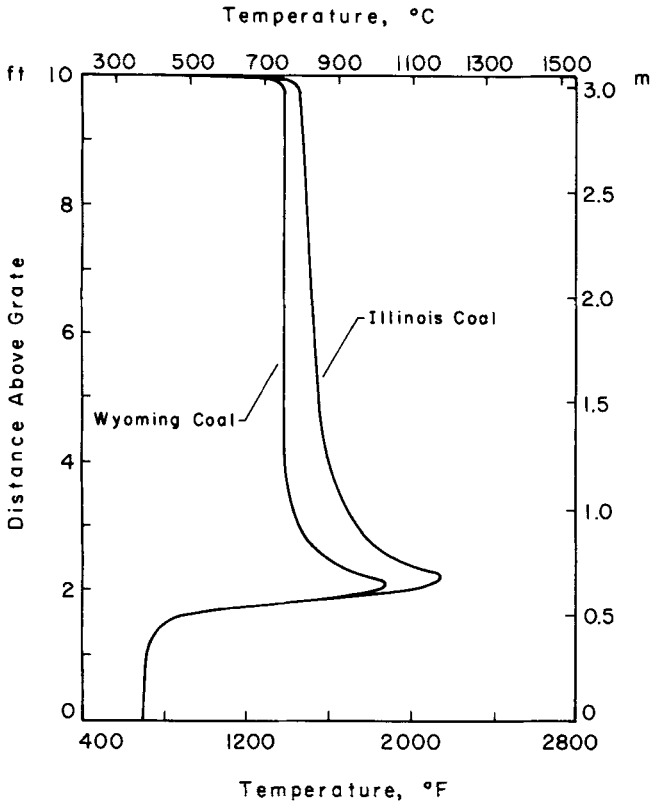

Fig. 5a. Temperature profiles calculated by SP model for operating conditions in Table 6 and $F°C/F°O_2 = 3.27$ for Illinois coal and 3.68 for Wyoming coal.

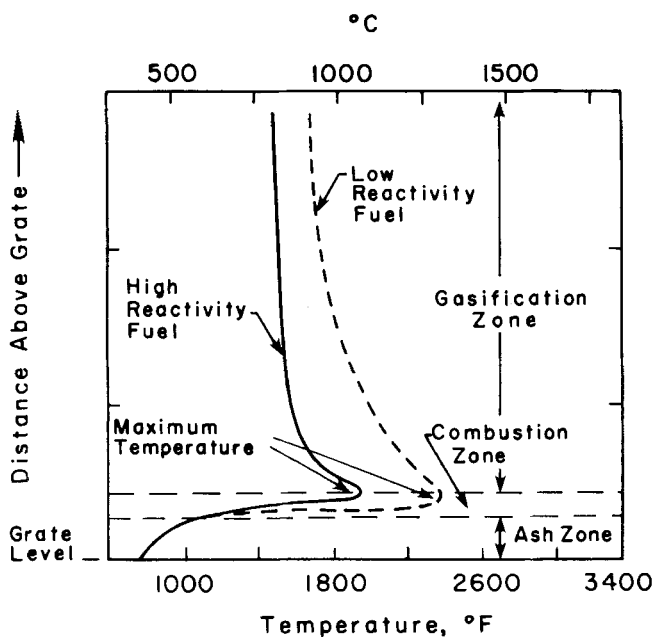

Fig. 5c. Temperature profiles with coals of different reactivity, as reported by Hebden (1975). No scale was given for distance above the grate.

Table 6. Operating Conditions Used in Simulation

Feed rate (Moe, 1973)	
Steam	0.5915 Kg/m²s (436.1 lb/ft² hr)
Oxygen	0.1546 Kg/m²s (114.0 lb/ft² hr)
Gas inlet temperature	371°C (700°F) (Hebden, 1973; Rudolph, 1972)
Operating pressure	25 atm (350 lb/in.²gauge) (Elgin and Perks, 1974; Lacey, 1967)

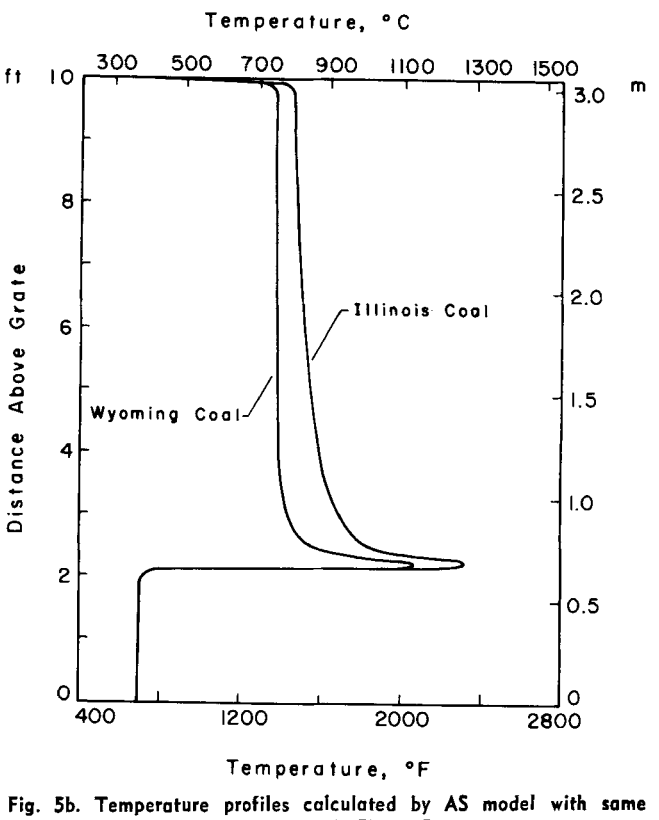

Fig. 5b. Temperature profiles calculated by AS model with same conditions as in Figure 5a.

Illinois and Wyoming coals, operated at the same steam-to-oxygen molar feed ratio of 6.8 (see Table 6). For ease of comparison, the curves were computed with conditions at the bottom such that both cases have the same position of the maximum temperature. The two coals are assumed to have identical combustion parameters, but the Wyoming coal is more reactive towards steam. The sharp temperature peak delineates the region in which the exothermic combustion reaction occurs. The temperature rise is greater for the Illinois coal because less of the heat which is generated is consumed by the endothermic gasification reaction.

The AS model predicts a higher and sharper maximum temperature for both coals than the SP model. In the SP model, the ash shell layer limits the diffusion of oxygen to the reaction sites and slows down the combustion reaction in comparison to the AS model. Except for this difference in the maximum temperature, the predictions by both models are essentially the same.

At the upper stage of the gasification reaction, the carbon-steam and carbon-carbon dioxide reactions slow down with falling temperature and appreciable reverse reactions and move towards equilibrium. This effect is more significant for Wyoming coal and contributes to the fact that the temperature profile for this high activity coal is more flattened than that for Illinois coal. The computed profiles are quite similar to those reported experimentally by Hebden (1975) and reproduced in Figure 5c. Quantitative comparison is not possible, since a complete set of coal properties and operating conditions were not given by Hebden, not was a scale provided for distance above the grate.

For a given coal, the maximum temperature in the reactor can be controlled by varying the steam-to-oxygen ratio in the feed. Figure 6 shows the results of such calculations for the Wyoming and Illinois coals using the AS model, together with curves reported by Rudolph (1972) and by Hebden (1975). The AS model has been chosen

for this calculation since it gives a higher maximum temperature than the SP model and thus provides a conservative prediction for the Lurgi gasifier; the AS model may be more appropriate than the SP model for Illinois and Wyoming coals, which will have small amounts of ash. These calculations were carried out for constant coal and oxygen input, but variable steam input. Rudolph's curve is the maximum temperature attainable, assuming that the residual carbon entering the combustion zone is converted entirely to carbon dioxide; he pointed out that this temperature is, in fact, never reached. It is interesting that Rudolph's maximum temperature has the same dependency on steam-to-oxygen ratio as the model calculations but lies above them, while Hebden's data lie below the model calculations for Illinois coal and at almost the same level as the model calculations for Wyoming coal. Clearly, either behavior can be accommodated within the model by changes in system parameters and operating conditions. The SP model predicts the same behavior for the maximum temperature as the AS model, except that the maximum temperature curve is lower by about 100°C (180°F).

Figures 7 and 8 show temperature and composition profiles by the SP model for the Wyoming coal, using the operating conditions recorded in Table 6 and a coal feed rate giving a fixed carbon-to-oxygen molar feed ratio of 3.6. The temperature profile computed from the AS model is also shown in Figure 7 for comparison. The feed rates of steam and oxygen are comparable to those given by Moe (1973), and the feed rate of fixed carbon is about 4% more than that of Moe. Gas compositions are normalized relative to the steam feed rate in moles. There is

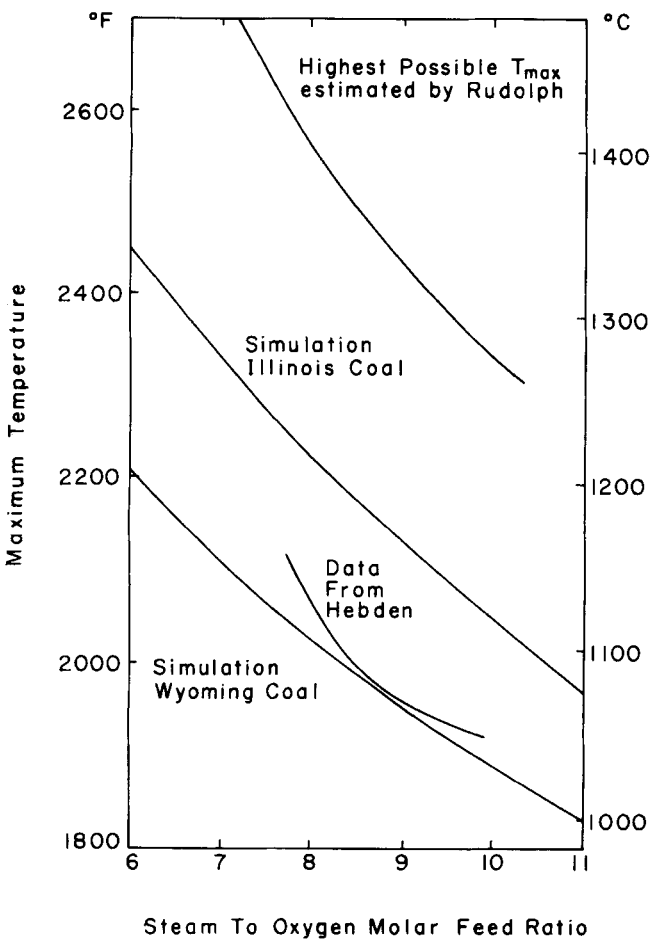

Fig. 6. Maximum temperature as a function of steam/oxygen ratio with oxygen feed rate in Table 6 and $F°C/F°O_2 = 3.3$.

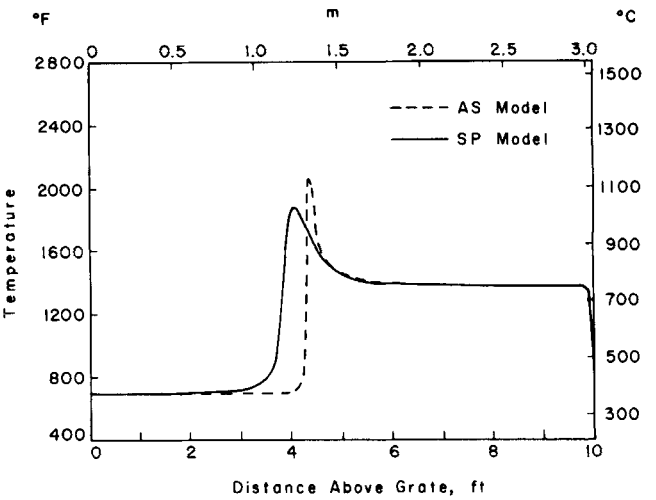

Fig. 7. Temperature profile with Wyoming coal for conditions in Table 6 with $F°C/F°O_2 = 3.60$.

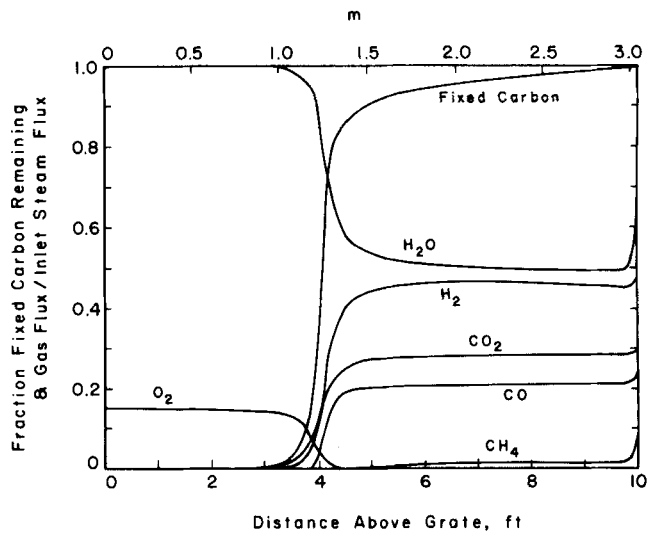

Fig. 8. Composition profiles with Wyoming coal for conditions of Figure 7.

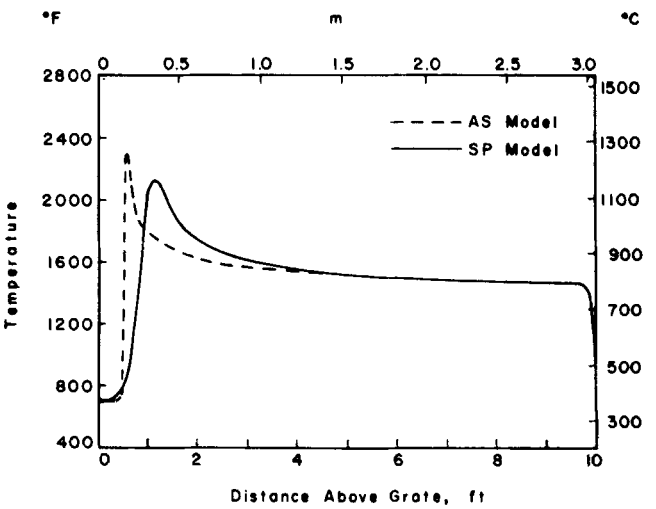

Fig. 9. Temperature profile with Illinois coal for conditions in Table 6 with $F°C/F°H_2O = 3.29$.

overlap between the combustion and gasification zones near the temperature peak, where both oxygen and water concentrations are changing rapidly. Gasification is mostly completed a short distance above the point where oxygen

Table 7. Product Gas Compositions On Dry Basis (% v/v). These Calculations are Based on the Distribution of Devolatilization Products in Table 3

	Simulation				Plant data		
	Wyoming coal		Illinois coal				
Component	Without boundary layer	With boundary layer	Without boundary layer	With boundary layer	Rudolph (1972)	Hoogendorn (1973)	Moe (1974)
H_2	42.5	43.1	43.9	43.6	38	39	37.9
CO_2	26.8	27.5	26.6	27.8	28	28	28.6
CO	21.5	20.3	22.2	21.0	24	22	20.3
CH_4	8.0	7.9	6.2	6.4	10	9	11.4
Others	1.2	1.2	1.1	1.2	0	2	1.9

is depleted. The AS model gives similar results except for the sharpening of the intensive reaction zone around the temperature peak. The devolatilization and drying zones occupy a very small distance at the top of the bed. Despite the slow rate of change, equilibrium is not attained at the top of the bed.

Figures 9 and 10 show similar calculations for the Illinois coal. The position of maximum temperature is much lower. Substantially less of the fixed carbon is removed in the narrow combustion zone, the region of gasification is wider, and the throughput of coal is reduced substantially. This reduction of throughput can be compensated for by increasing the oxygen feed rate, but it would then be necessary to increase the steam feed rate as well in order to control the peak temperature.

Boundary Layer. Because of the heat loss, the gasification efficiency in the boundary layer is significantly less than that in the core, and thus a larger amount of fixed carbon remains in the ash at the bottom of this region. In the simulations carried out here, this carbon in the boundary-layer ash comprised 10 to 30% of the boundary-layer feed carbon and was thus the major source of fixed carbon in the ash from the reactor. The temperature profile was almost independent of the operating conditions, as was the steam production rate in the jacket. The temperature reached its maximum rapidly and dropped gradually, approaching the saturation temperature of steam in the jacket (434°F, 223°C) owing to the heat loss and the endothermic gasification reaction. Calculated jacket steam production was 12 to 13% of process steam with Wyoming coal and 15 to 16% with Illinois coal using the SP model. An 0.8% lower production rate of steam was predicted with the AS model for both coals.

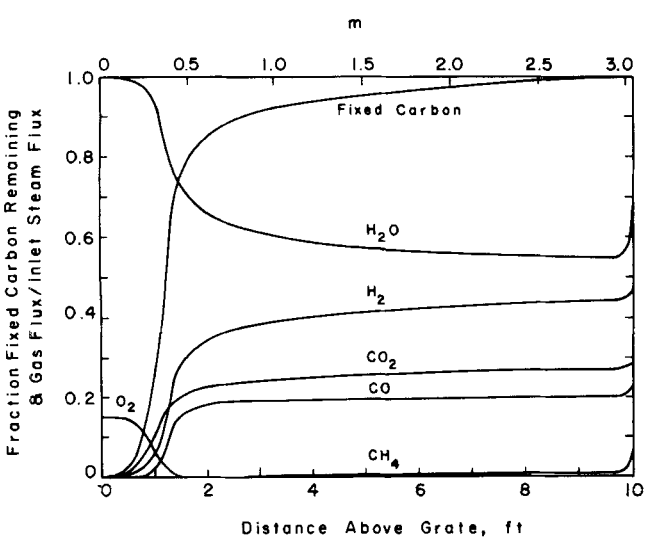

Fig. 10. Composition profiles with Illinois coal for conditions of Figure 9.

Composition of Product Gas. The composition of the effluent gas was computed for the Wyoming and Illinois coals at the operating conditions used to construct Figures 8 and 10, respectively, with and without the contribution of the boundary layer. The composition including the boundary layer is not much different from the composition without it for both coals, but there is slightly more carbon dioxide and slightly less carbon monoxide in the gas stream when the boundary layer is included because of the lesser extent of gasification in this zone.

The results tabulated in Table 7 were computed using the first assumption about volatiles and the product distribution in Table 3. Data of Rudolph (1972), Hoogendorn (1973), and Moe (1973) are also included in the table for comparison; these data are used because their steam-to-oxygen molar feed ratios are comparable to the ratio employed for the calculation here, though quantitative comparison in the absence of a detailed characterization of the coal and complete operating data is impossible. It is interesting to note that the major differences in all cases is that the simulation predicts an excess of hydrogen and too little methane in the product gas compared to the data. This difference is consistent with the belief that tar from volatile matter is cracked and that a methanation reaction between hydrogen and super active carbon takes place under conditions of devolatilization to produce approximately one third of the methane from the reactor. Such reactions have little effect on combustion and gasification in the reactor and can be accommodated in the simulation of the upper zone of the reactor.

The product distribution for the Illinois coal was also computed using the second assumption for the devolatilization. The ultimate analysis and laboratory devolatilization data are given in Table 8; the ultimate analysis is for the Illinois coal, but devolatilization data for this coal are not available, so data of Loison and Chauvin (1964) (for a coal with a similar proximate and ultimate analysis) were used. For this calculation, the overall mass balance must be satisfied for every element and the overall energy balance closed to within 3%. The computed product distribution is shown in Table 9; the simulation is in even closer agreement with the Table 7 plant data, though the methane production is still slightly low. This small discrepancy may simply reflect differences in coals, or it may result from failing to account for the methanation reaction between hydrogen and superactive carbon.

Data are shown in Table 10 for the product gas composition from a Lurgi gasifier in Westfield, Scotland operating with Illinois coal, together with simulation results

for the same nominal feed ratio conditions. There is some uncertainty about the proper value of the oxygen feed rate, because the purity of the product from the oxygen plant was not specified. The agreement between the simulation and the plant data is quite good for this case as well, which is at a much higher steam-to-oxygen ratio than the data in Table 7. The largest discrepancy is in the carbon monoxide composition of the product gas, which may reflect, in part, the uncertainty in the oxygen flow rate as well as the treatment of the volatiles.

Table 8. Ultimate Analysis of Illinois Coal and Distribution of Volatiles For a Similar Coal

Ultimate analysis (Elgin and Perks, 1974)

Elements	Percent by weight (dry basis)
C	71.47
H_2	4.83
N_2	1.35
S	3.13
Cl	0.06
Ash	10.14
O_2 (difference)	9.02
Total	100.00

Distribution of devolatilization product (Loison and Chauvin, 1964)

	Percent by weight
Coal gas	34.3
Tar, oil plus phenol	51.5
Chemical water	14.2

Distribution of coal gas (% v/v) as in Table 3.

Table 9. Simulated Product Gas Composition (% v/v) for Illinois Coal Using Data in Table 8

	Without boundary layer	With boundary layer
H_2	41.3	41.0
CO_2	26.3	27.4
CO	21.0	20.0
CH_4	9.2	9.4
H_2S	1.0	1.0
N_2	0.5	0.5
C_2H_6	0.7	0.7

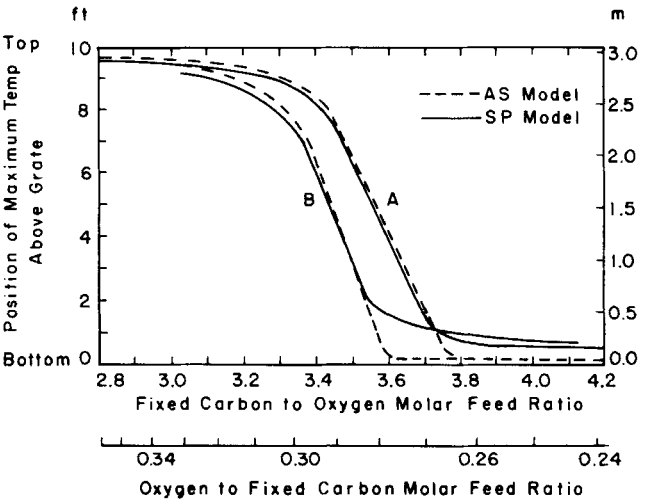

Fig. 11. Position of maximum temperature as a function of fixed carbon to oxygen molar feed ratio for Wyoming coal. Curve A: steam and oxygen feed rates as in Table 6. Curve B: steam and oxygen feed rates twice those in Table 6.

Reactor Performance

The primary use of a simulation model is to allow computer experiments to be carried out in order to study the effect of changes of raw materials and design and operating conditions on reactor performance. We show here the results of such an experiment, using the Wyoming coal described in Tables 4 and 5.

Figure 11 shows the location of the maximum temperature in the adiabatic core as a function of the molar feed ratio of fixed carbon to oxygen. Here, the coal feed rate is varied, and the oxygen and steam feed rates are kept constant at a steam-to-oxygen molar feed ratio of 6.8. Curves A are obtained with the operating conditions given in Table 6 and curves B with steam and oxygen feed rates twice those in Table 6. The relative positions of curves A and B show that it is necessary to supply higher oxygen and steam-to-coal ratios to process an increased coal rate if the maximum temperature is to be maintained at the same position in the reactor. This is because with

Table 10. Product Gas Compositions on Dry Basis (% v/v). Simulation and Plant Data from a Lurgi Gasifier in Westfield, Scotland

Compound	Simulation devolatilization product as in Table 3		Simulation tar cracking assumption		Westfield plant data (Elgin and Perks, 1974)
	Without boundary layer	With boundary layer	Without boundary layer	With boundary layer	
CO_2	32.8	33.7	32.0	32.9	31.2
CO	15.4	14.4	14.8	13.8	17.3
H_2	45.0	45.0	42.5	42.4	39.1
CH_4	5.7	5.8	8.5	8.6	9.4
C_2H_6	1.1	1.1	0.7	0.7	0.7
H_2S			1.0	1.0	1.1
Inert			0.5	0.5	1.2

Operating conditions (Simulation): oxygen feed rate = 0.1546 Kg/m² s (114.0 lb/ft² hr); gas inlet temp = 371°C (700°F); operating pressure = 25 atm; steam/oxygen feed ratio = 9.6; fixed carbon/oxygen feed ratio = 2.73

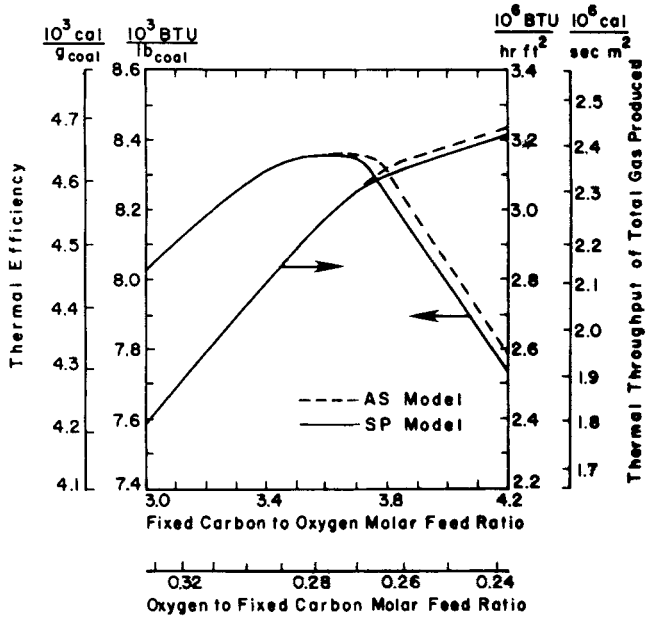

Fig. 12. Thermal efficiency and thermal throughput of gas produced as a function of fixed carbon to oxygen molar feed ratio for conditions of curve A in Figure 11; adiabatic core only.

an increased throughput, the residence time for gasification is reduced proportionally if the position is kept constant. Thus, it is necessary to supply more oxygen to compensate for this reduction in the extent of gasification. Since the gasifier is operated with more combustion and less gasification, the gasification efficiency is lowered as the throughput is increased. This calculation does show, however, that when there is an increased demand of the fuel gas, the reactor can meet this demand easily with an increase in the feed rates of coal and gaseous reactants, but with an increase in pressure drop.

The location of the maximum temperature, which defines the combustion zone, is an important parameter in defining the efficiency of reactor operation. The fixed carbon must be either gasified, combusted, or removed from the reactor in the ash. If the combustion zone is too low in the reactor, then there will be insufficient combustion and an excess of unreacted carbon in the ash. If the zone is too high, there may be insufficient gasification coupled with too much combustion. Predictions of the location of the maximum temperature by the AS and SP models are not very different, except when the fixed carbon-to-oxygen ratio is high and the position of the maximum temperature is near the bottom of the reactor. In that case, the SP model does predict a higher position in the reactor for the combustion zone. As we shall see, even this difference does not make the predictions of the performance of the reactor by the two models differ appreciably; this is because the difference between the two ash models is only appreciable when the reaction is intensive enough to be controlled by diffusion, and this intensive zone is very narrow for either model compared to the height of the reactor.

For the two cases shown in Figure 11, the value of the maximum temperature is substantially independent of its location in the reactor, never differing by more than a few percent from 1 165°C (2 130°F). The unreacted carbon in the ash ranges from less than 0.001% for a high location to more than 5% for a location near the bottom of the reactor. The SP model gives a little more unreacted carbon in the ash than the AS model. The temperature of the gas at the top of the gasification zone in the adiabatic core increases from 753° to 838°C (1 387° to 1 540°F) as oxygen to fixed carbon feed rate increases. The gas temperature remains about 760°C for $F°_{O_2}/F°_C < 0.29$. At an oxygen-carbon ratio above 0.35, unreacted oxygen appears in the gas leaving the gasifier.

Figure 12 shows the chemical energy throughout and thermal efficiency of the gas produced in the adiabatic core for the conditions corresponding to case A in Figure 11, and Figure 13 shows the same calculations when the effect of the boundary layer is included. Calculations are done with the AS and SP models for both figures, and both models give similar results for the reasons noted previously. Comparison of Figures 12 and 13 shows that the efficiency is lowered by up to 3% by the presence of the boundary layer, but the dependency of reactor performance on the molar feed ratio of fixed carbon to oxygen is unchanged. It is evident that the adiabatic core dominates the performance of the Lurgi gasifier.

The thermal efficiency reaches a maximum at a carbon to oxygen molar feed ratio of about 3.70, but the efficiency curve is flat and remains high for carbon to oxygen ratios from 3.45 to 3.70. This behavior results from differences in the extent of the methanation reaction during gasification. Methanation (3) is the only exothermic reaction of the three gasification reactions, and it leads to a beneficial trade off from sensible heat to chemical heat. At a carbon/oxygen ratio of 3.45, the position of the maximum temperature is so high that the time available for the methanation reaction is short, and there is little methane formed by gasification. On the other hand, more methane is formed by gasification at a ratio of 3.70, thus maintaining the thermal efficiency at a high level despite the increased throughput of coal. Hence, the methanation reaction does play an important role in the performance of the gasifier by reducing the amount of oxygen required and increasing the throughput of the reactor. In terms of thermal efficiency and throughput of the total gas produced, the optimum operation lies near the carbon/oxygen ratio of 3.70. A drastic drop in performance occurs below a ratio of 3.0, when excess oxygen appears in the exit gas. It is interesting to note that the maximum in thermal efficiency occurs at the greatest slope of the

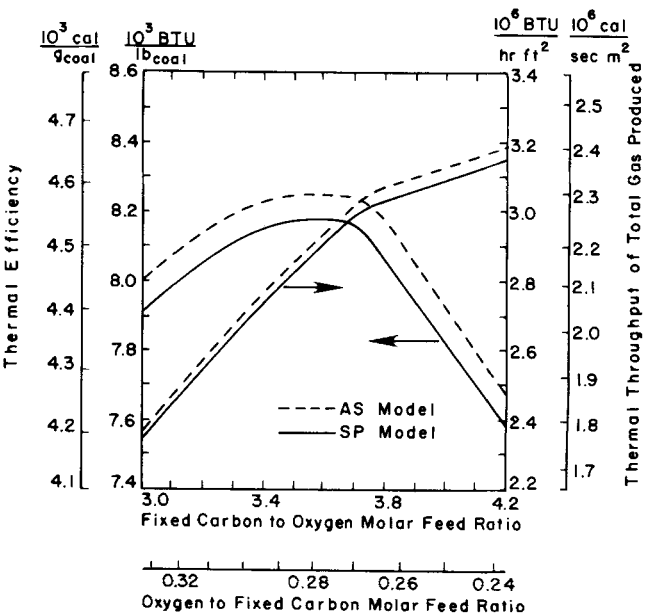

Fig. 13. Thermal efficiency and thermal throughput of gas produced as a function of fixed carbon to oxygen molar feed ratio for conditions of curve A in Figure 11; adiabatic core and boundary layer.

position of the maximum temperature-fixed carbon to oxygen molar feed ratio curve in Figure 11, suggesting a possible sensitivity in controllability under these operating conditions.

Effect of Blast Temperature on Gasifier Operation

The blast temperature, or temperature of the feed gas, at which the Lurgi gasifier operates has been reported as ranging from 232° to 510°C (450° to 950°F) (Krieb, 1973; Rudolph, 1972; Hebden, 1975; Ricketts, 1963; Papic, 1976). The blast temperature can be an important parameter in determining gasifier performance. We have studied the effect of blast temperature on the performance of an oxygen blown Lurgi gasifier with the Wyoming coal described in Tables 4 and 5, using the other operating conditions in Table 6. All calculations were carried out for the adiabatic core using the AS model.

Figure 14 summarizes the properties of the point of maximum thermal efficiency for each blast temperature. It is evident that for the Wyoming coal the reactor can be operated at temperatures above 260°C (500°F) without appreciable loss of unreacted carbon in the ash, but that below this temperature the carbon in the ash increases greatly. The ratio of fixed carbon to oxygen for maximum thermal efficiency is an increasing function of blast temperature above 232°C (450°F) because the increased sensible heat means less combustion is required to sustain the endothermic gasification reactions. The increase in this ratio at lower temperatures results from the loss of large amounts of unreacted fixed carbon.

The height above the grate of maximum temperature as a function of blast temperature is of particular processing interest. As the blast temperature is decreased, more of the reactor space is required for the light up of the combustion reaction, and the space available for gasification is diminished. At blast temperatures below 232°C, most of the reactor space is required for light up and combustion, and the reactor cannot be operated efficiently.

It will be true in general that there will be a critical blast temperature, dependent on the reactivity of the coal, below which efficient operation cannot be carried out because of excessive carbon loss in the ash and insufficient extent of gasification. It is evident from Figure 14 that prediction of the reactor performance near the critical blast temperature will require very precise knowledge of combustion kinetics because of the effect of the long light up distance, while the performance is less sensitive to the combustion kinetics at higher blast temperatures.

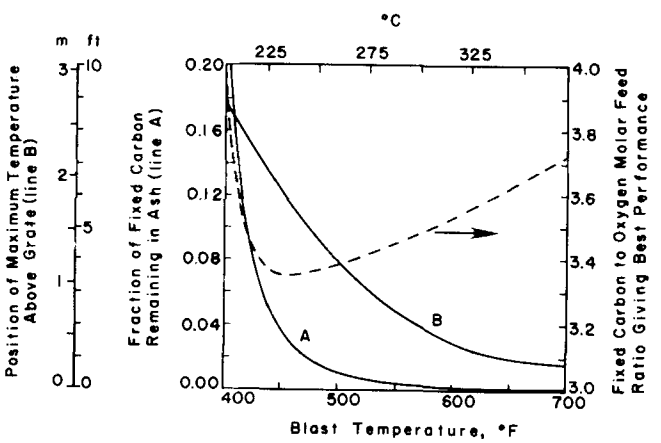

Fig. 14. Effect of blast temperature on performance of the adiabatic core for oxygen blown Lurgi gasifier with Wyoming coal for operating conditions in Table 6.

APPLICATION TO THE OXYGEN BLOWN SLAGGING GASIFIER

The model is also applicable to the slagging moving-bed gasifier. The slagging gasifier at Solihull, England, is described by Hebden et al. (1964) and Lacey (1967), and the slagging gasifier at the ERDA Energy Research Center in Grand Forks, North Dakota, is described by Ellman and Johnson (1976), Ellman et al. (1977), and Johnson et al. (1977). In these gasifiers, steam and oxygen are injected radially through feed ports, called tuyers, which are located above the hearth plate. Below the tuyers, the ash slag accumulates as a pool before leaving the reactor through the slag tap hole in the hearth. A slag tap burner is installed underneath the hearth to prevent resolidification of the slag in the accumulation zone. These two pilot scale gasifiers have been used successfully to gasify coals at elevated pressure. We present here the results of applying the simulation model to the slagging gasifier at Solihull. This reactor has been chosen because it has a larger diameter than the reactor at Grand Forks, and hence the wall cooling effect is expected to be small.

It is necessary to make some small changes in the model for simulation of the slagging gasifier. It is assumed that the molten slag dripping from the solids at a temperature above 1 500°C (2 730°F) does not come to equilibrium with the cold gas entering the reactor from the tuyers. The simulation is started at the tuyer level, where the burner gas is taken to be at the temperature at which slag leaves the reactor, 1 500°C, and is mixed with the entering steam and oxygen. These modifications eliminate the need to include detailed mass and energy balance calculations for the region from the burner to the tuyer level, where most of the uncertainties are located. Above the tuyer level, the reactor has a refractory wall, and the gasifier is assumed to be adiabatic.

Simulation Calculations

Calculations were done to simulate runs at Solihull for Avenue coke, test 54, and Donisthorpe D.S. nuts (bituminous coal), test 67 (Lacey, 1967). Test 67 was chosen because the duration of this pilot experiment was the longest

Table 11. Properties of Coals Used in Two Tests of the Slagging Gasifier at Solihull, England (Lacey, 1967)

	Test No. 54 Avenue coke	Test No. 67 Donisthorpe D.S. nuts
Estimated composition (Moisture free basis, wt %)		
Fixed carbon	82.34	54.50
Volatile matter	10.11	38.15
Ash	7.55	7.35
Ultimate analysis (Moisture free basis, wt %)		
C	88.0	71.3
H	0.75	5.0
N	1.05	1.55
S	1.15	1.45
Cl	0.05	0.15
O	1.45	13.2
Ash	7.55	7.35
Weight fraction of moisture as charged	9.45	12.70
Liquid ash flow temperature, °C (°F)	1 345(2 450)	1 330(2 430)

TABLE 12. OPERATING CONDITIONS FOR TWO TESTS ON THE SLAGGING GASIFIER AT SOLIHULL, ENGLAND (LACEY, 1967)

	Avenue coke test No. 54	Donisthorpe D.S. nuts test No. 67
Operating pressure, atm (lb/in.²gauge)	21.4 (300)	21.4 (300)
Coal feed rate (moisture and ash free) Kg/s m² (lb/hr ft²)	0.698 (515)	1.33 (980.4)
Gas feed rate, Kg/s m² (lb/hr ft²)		
Oxygen	0.481 (354.6)	0.633 (466.6)
Steam	0.317 (233.4)	0.391 (288.3)
Steam/oxygen (mole/mole)	1.17	1.10
Gas feed temperature, °C(°F) (assumption)	371 (700)	371 (700)
Slag tap burner gas feed rate by element mass balance Kg/s m² (lb/hr ft²)		
Carbon	0.00787 (5.80)	0.00787 (5.80)
Hydrogen	0.00288 (2.12)	0.00288 (2.12)
Oxygen	0.0774 (57 04)	0.0726 (53.48)
Nitrogen	0.177 (130.72)	0.177 (130.72)

reported (81 hr). Test 54 was chosen because reactor performance with the Avenue coke, which has very little volatile matter, should depend mostly on the combustion and gasification reactions and very little on the devolatilization. Thus, the simulation results for the coke should provide the best information as to whether the model predictions for the combustion and gasification reactions in the slagging gasifier are in agreement with experiment.

Analysis data for these two coals are given in Table 11. Coal proximate analyses were not reported in the published paper, and we estimated the amount of fixed carbon in each coal from plant data; this is possible, since the amount of fixed carbon can be obtained from the stoichiometries of the combustion and carbon-steam reactions.

Table 12 shows the operating conditions for both tests. Because of the addition of the gas from the slag tap burner, the actual steam to oxygen molar feed ratio for the gas stream entering the combustion zone is slightly different from the ratio given in the table. The coal throughput is about three times that in the Lurgi reactor. Higher throughput has been achieved in pilot plant operation, and it has been claimed that the increased coal throughput could reach four to seven times the throughput of the Lurgi (Lacey, 1967; Hebden et al., 1964). This increase is an important potential advantage of the slagging gasifier over the Lurgi.

Reactivity data are not available for either coal, and we used the data for the Illinois and Wyoming coals as being representative of coals of widely varying reactivity. The computed maximum temperature using the properties of the Donisthorpe coal is shown in Figure 15, together with the measured maximum temperature in the two tests. $\lambda = 2.0$ means the combustion product of carbon is 100% carbon monoxide, and $\lambda = 1.33$ means 50% carbon monoxide. Since the combustion temperature is very high, carbon monoxide is likely to be the major combustion product. The predicted maximum temperatures for both reactivities are sufficiently high to make ash drip

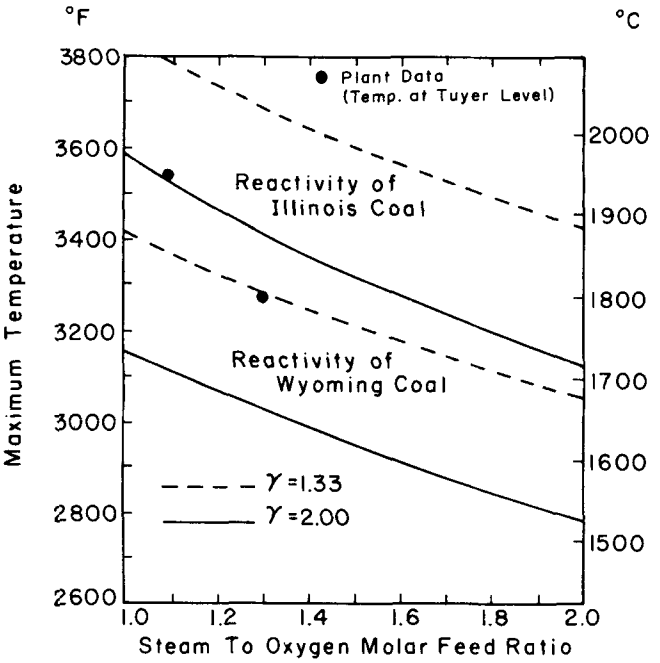

Fig. 15. Maximum temperature in slagging gasifier as a function of steam/oxygen ratio for Donisthorpe coal with operating conditions except steam feed rate as in Table 12.

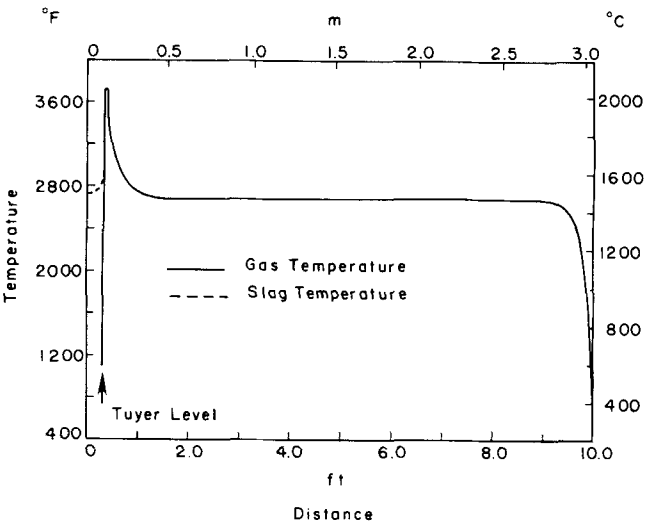

Fig. 16. Temperature profile calculated for Donisthorpe coal with operating conditions in Table 12.

off as liquid slag; the liquid ash flow temperatures are given in Table 11. The predictions of product gas composition and temperature and reactor performance are the same for both reactivities. The maximum temperature for Illinois coal reactivity is in closer agreement with the reported value, and we will thus present only the results obtained using the reactivity data of Illinois coal with $\lambda = 2.0$. The typical devolatilization data in Table 3 were used.

The predicted product gas compositions for the Avenue coke and the Donisthorpe coal, together with the pilot plant data, are given in Table 12. The prediction is in good agreement with the plant data for the Avenue coke. For Donisthorpe coal, however, the prediction shows less hydrogen and more carbon monoxide than the plant data. Prediction of too little hydrogen is consistent with the Lurgi calculations in Table 7 and is probably because of

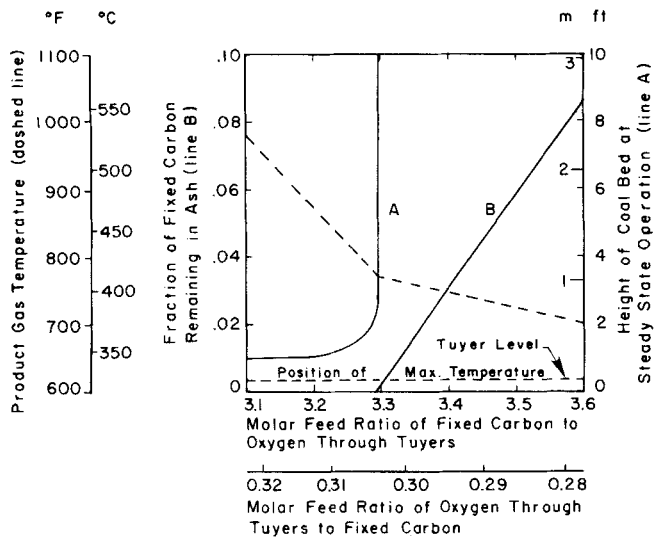

Fig. 17. Product gas temperature, carbon in ash, and coal bed height required to maintain maximum temperature at tuyere level as a function of fixed carbon to oxygen molar feed ratio for Donisthorpe coal with operating conditions except coal feed rate as in Table 12.

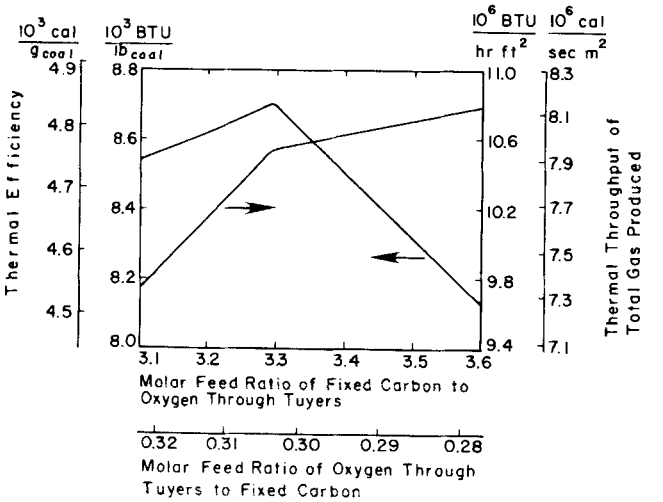

Fig. 18. Thermal efficiency and thermal throughput of gas produced as a function of fixed carbon to oxygen molar feed ratio for Donisthorpe coal with operating conditions except coal feed rate as in Table 12.

the error in the distribution of devolatilization products, which cannot satisfy mass balances on the individual elements. This error is diminished for the coke, since the amount of volatile matter is rather small.

The computed temperature profile for Donisthorpe coal under the operating conditions in Table 12 is shown in Figure 16. The temperature of the gas increases sharply at the tuyer entrance to a maximum value at $z = 90$ mm (0.3 ft) in the combustion zone, decreases rapidly because of the endothermic reduction reactions, and then remains at a constant temperature until the sensible heat is consumed for drying and heating of the coal at the top of the bed. The product gas temperature was predicted to be 405°C (760°F), which is only slightly higher than the reported gas temperature (350° to 400°C) from the pilot plant (Lacey, 1967). The combustion and gasification reactions are practically completed at a bed height of 0.45 m (1.5 ft). Thus, the simulation shows that a large portion of the reactor is not used as reaction space in the slagging gasifier. This observation is consistent with carbon profiles reported by Johnson et al. (1977).

Table 13. Product Gas Compositions on Dry Basis (% v/v). These Calculations are Based on the Distribution of Devolatilization Products in Table 3

	Donisthorpe coal		Avenue coke	
	Simulation	Plant data	Simulation	Plant data
CO	66.4	61.3	71.9	70.45
H_2	24.0	28.05	25.8	27.25
CO_2	0.9	2.55	0.4	1.85
CH_4	7.3	7.65	1.6	0.45
Others	1.4	0.45	0.3	0.0

The liquid slag formed in the intensive reaction zone drips off the particle and meets the incoming cold feed gas. We have estimated the travel time for the liquid slag from the lower end of the intensive reaction zone to the level below the tuyers to be much shorter than the time required for the resolidification of the slag in the coal bed. The slag temperature profile below the tuyer level shown in Figure 16 is not computed from the model but is simply estimated from the known exit condition.

If the steam to oxygen molar feed ratio is increased and/or the gas feed temperature is reduced, the ignition distance for combustion becomes longer. If the distance exceeds some maximum tolerable distance, then slagging operation is impossible, and ash clinkers will be formed by the resolidification of ash slag. Thus, the feed conditions must be controlled to keep the combustion zone just above the hearth. The slagging gasifier differs from the dry ash Lurgi in this regard, since the maximum temperature zone in the Lurgi may be nearly a meter (several feet) above the grate, with the space between filled with ash.

Performance of the Slagging Gasifier

The position of the maximum temperature must be controlled near the tuyer level so that the travel time of liquid slag through the cold feed gas is short enough to prevent slag solidification. The hot spot has been observed around the tuyer level in successful pilot plant operation (Lacey, 1967). If such control can be achieved, Figures 17 and 18 show how the important parameters depend on the coal feed rate at steady state. The operating conditions other than the coal feed rate are given in Table 12 for the Donisthorpe coal. It is assumed for this calculation that the coal feed rate can be adjusted independently of the gas feed rate.

There is an optimum feed ratio of fixed carbon to oxygen of 3.3. At this optimum ratio, there is almost no unburned carbon loss, and the product gas temperature is 405°C (760°F). If the fixed carbon rate is increased above this ratio, carbon loss must increase, and the thermal efficiency will decrease. The position of maximum temperature in the bed always remains at the tuyer level with carbon rates above the optimum.

If the fixed carbon rate can be separately controlled and is decreased below the optimum level, the model predicts that the maximum temperature zone will rise well above the tuyer level, which could lead to freezing of the slag. It may be possible to operate in this region of decreased carbon rate with a very thin bed, however, and to maintain the maximum temperature zone at the tuyer level. The bed level that is required to maintain the maximum temperature at the tuyer is shown in Figure 17. The product gas temperature rises rapidly in the region where a thin bed is required, and this is detrimental to thermal efficiency.

The effects of the chemical heat loss in the unreacted carbon in the ash and the sensible heat loss in the product gas are shown in the thermal efficiency and throughput curves in Figure 18. The sharp maximum in the efficiency curve occurs just above the feed ratio at which the bed height must be greatly decreased to maintain the hot zone at the tuyer level. This suggests a possible controllability problem for feed fluctuations when operating at the optimum.

If the reactivity for the Wyoming coal is used instead of the data for the Illinois coal, the curves in Figures 17 and 18 are unchanged. Thus, in contrast with the Lurgi reactor, the overall performance of the slagging gasifier does not depend on the coal reactivity. The higher temperatures encountered mean that thermodynamic equilibrium is reached even for the low reactivity coal at the top of the gasification zone. The optimal fixed carbon to oxygen molar feed ratio for the slagging system is obtainable from the stoichiometries and equilibria of the carbon-oxygen reaction to form carbon monoxide and of the carbon-steam reaction. The magnitude and location of the maximum temperature cannot be computed without the rate and transport model, however.

DISCUSSION

Factors Determining the Magnitude of the Maximum Temperature

The maximum temperature attained is an important variable in determining the overall operating conditions of the moving-bed coal gasifier. A gasifier is designed to give particular ash characteristics at the bottom of the reactor. In the Lurgi gasifier, the grate at the bottom of the reactor (see Figure 1) only processes powdered ash, so that the maximum temperature must be controlled below the melting or sticky point of the ash for the particular coal being processed. In the slagging gasifier, ash is taken away as molten slag, and the maximum temperature must be controlled above the fluid point of the ash. The GEGAS gasifier can process ash clinker and can be operated with a maximum temperature above that of the Lurgi, but below slagging conditions. Thus, for successful operation of a moving-bed gasifier, it is essential to know how to control the maximum temperature within the operable range.

There are several factors influencing the maximum temperature, including:

1. Steam to oxygen molar feed ratio.
2. Temperature of steam and oxygen (or air) feed (blast temperature).
3. Mineral composition of ash and adherence of ash to unburned coke.
4. Size of particles in the intensive combustion zone.
5. Axial thermal diffusion.
6. Ratio of the primary combustion products, carbon monoxide and carbon dioxide.
7. Extent of gas phase combustion of carbon monoxide and hydrogen.
8. Reactivity of coal to water, hydrogen, and carbon dioxide.

Only the first two factors are directly controllable. Control of the steam-to-oxygen feed ratio is standard practice in the actual operation of moving-bed gasifiers. The blast temperature has only a weak influence on the maximum temperature in the bed, as long as it is high enough to cause light up of the combustion reaction near the bottom of the reactor.

The other factors cannot be controlled directly, but their influence on the maximum temperature can be computed or estimated. The effect of the third factor, the ash, was clearly displayed by using both the AS and SP models as the possible extremes of ash behavior. The average particle size in the combustion zone depends primarily on the initial size of coal particles, but some change of particle size occurs during devolatilization; this size change will influence the maximum temperature because it will change the diffusion rate controlling the rapid combustion reaction.

The extent of axial thermal diffusion is proportional to the average particle diameter in the bed because the heat conductivities due to radiation and axial turbulent diffusion are proportional to the average particle size. In the Lurgi gasifier, since powder ash is produced from the combustion reaction and the size of the ash particle is very small, the axial thermal diffusion from the hot combustion zone to the ash zone is expected to be very low. In the GEGAS gasifier, however, large ash clinker could promote this thermal diffusion. In all cases, the thermal diffusion will lower and widen the maximum temperature peak, with the degree of this effect depending on the system employed. The effect is not expected to be a major one, as indicated by the Peclet numbers computed earlier, and it is not included in the model calculations.

The sixth and seventh factors relate to the heterogeneous and gas phase combustion reactions. It is widely believed that both carbon monoxide and carbon dioxide are primary combustion products of carbon. There are limited data concerning the ratio of these combustion products, however, which can be used over the wide range of temperature variation and at the high pressure experienced in moving-bed gasifiers; the available data are used to calculate the model parameter λ, which represents this product ratio. Gas phase combustion of carbon monoxide and hydrogen is not considered in the model. The extent of gas phase combustion depends on the reaction rate relative to the heterogeneous reactions, and the homogeneous reaction rate is unlikely to be comparable. Were the homogeneous combustion and heterogeneous gasification rates comparable, then the gasification products carbon monoxide and hydrogen would react in the presence of oxygen in the gas phase to form carbon dioxide and steam; in terms of temperature rise, this is equivalent to Rudolph's calculation of the maximum temperature curve in Figure 6, which is based on the assumption that all oxygen reacts with carbon to form carbon dioxide before any gasification reaction takes place. Such high temperatures are not observed in practice. Furthermore, attainment of such high temperatures because of significant gas phase combustion would be independent of coal type and reactivity, in contrast to the known differences between high and low activity coal such as shown in Figure 5. This observation is consistent with recent calculations of Edgar et al. (1976).

The last factor, coal reactivity, is important in that a high reactivity coal will give a lower maximum temperature than a low reactivity coal for the same blast conditions because of the endothermicity of the gasification reactions. This means, in practice, that high and low activity coals will require different blast conditions in order to operate at the same maximum temperatures. The effect of the factors from 3 to 7 is appreciable only in the intensive zone near the maximum temperature and is minor on the model predictions of the overall reactor performance.

Validity of the Water-Gas Shift Equilibrium Assumption

In order to test the validity of the assumption of equilibrium of the water-gas shift reaction, we modified the model to include the rate expression for this reaction and repeated some calculations for the Lurgi reactor with Illinois coal. In the absence of reactivity data for the water-gas shift reaction catalyzed by Illinois coal, we used the published data with charcoal (Long and Sykes,

1948) and with coke (Wen, 1972). It is expected that reactivity with charcoal will provide a lower bound, since the catalytic effect of coal char should be higher than that of charcoal.

The calculations showed that there was no appreciable difference in predictions for the adiabatic core between calculations using the charcoal reactivity for the water-gas shift reaction and those assuming equilibrium. Somewhat different gas compositions were predicted for the colder boundary layer, but the difference was small and further diminished when added to the gas from the adiabatic core to determine overall product gas composition. The computing time was increased by including the water-gas shift kinetics without appreciable change in the predictive ability of the model.

CONCLUSIONS

A simulation model of moving-bed coal gasification has been compared to plant data and shown to be in good agreement. The model is based on mass and energy balances, reaction and transport rates, and fundamental thermodynamic relations. The model can be used to predict the effects of changes in operating parameters and feed properties on reactor performance.

The heat loss through the wall to the jacket in the Lurgi gasifier has little effect on the overall performance of the 12 ft diameter reactor, but it does lead to more unburnt carbon in the ash and lower thermal efficiency relarive to an adiabatic reactor with the same feed ratios and throughput rates.

Lurgi gasifier performance is sensitive to the blast temperature. Below a critical blast temperature which is about 450°F (232°C) for combustion parameters assumed for the Wyoming coal, the location of the combustion zone will be very high above the grate, and carbon loss in the ash will be excessive.

The overall performance of the slagging gasifier is independent of coal reactivity and can be determined from stoichiometric and equilibrium calculations. The rate and transport model are required to compute the location and magnitude of the maximum temperature. The position of the maximum temperature must be maintained near the tuyer level to ensure that the travel time of liquid slag through cold feed gas is shorter than the cooling time required for solidification of liquid slag. At carbon-to-oxygen feed ratios below a critical value that is close to the optimum ratio, it may be necessary to operate with a very thin coal bed to maintain the hot zone at the tuyer level.

ACKNOWLEDGMENT

This research was supported in part by the Electric Power Research Institute. We are grateful to L. F. Atherton and M. J. Gluckman of EPRI, D. E. Woodmansee of GE, and S. C. Smelser of Fluor for helpful discussions and suggestions of relevant literature.

NOTATION

A = effective wall surface area per unit volume of the boundary layer
a = oxygen to steam molar feed ratio
b = fixed carbon to steam molar feed ratio
C_c° = initial concentration of fixed carbon in the particle
C_{pash} = mass heat capacity of ash
C_{pi} = molar heat capacity of component i
D_i = bulk gas diffusivity of gas species i
$D_{e,i}$ = effective diffusivity of gas species i in the core of a particle
$D_{M,i}$ = effective diffusivity of gas species i in the shell of a particle
d°_p = original particle diameter
d_p = particle diameter
E_i = activation energy for reaction i
E_v = activation energy for devolatilization
f = mass fraction of volatile matter remaining in coal particle
f_{ash} = weight fraction of ash in the coal
F°_c = molar feed flux of fixed carbon
$F^\circ_{H_2O}$ = molar feed flux of steam
$F^\circ_{O_2}$ = molar feed flux of oxygen
F_G = total molar flux of gas phase
G°_{coal} = coal mass feed flux
h = overall heat transfer coefficient from the boundary layer to the jacket
H_G = heat capacity flux of gas phase
H_S = heat capacity flux of solid phase
ΔH°_i = reference enthalpy change of reaction i for equilibrium data
ΔH_i = enthalpy change of reaction i
k_e = radial effective thermal conductivity of the bed
$k_{i,o}$ = Arrhenius constant for intrinsic reaction i
$k_{p,i}$ = mass transfer coefficient of gas species i through gas film surrounding a particle
$k_{r,i}$ = intrinsic reaction rate coefficient for reaction i
$k_{v,o}$ = Arrhenius constant for devolatilization
K°_i = preexponential factor in equilibrium constant for reaction i
l = thickness of boundary layer
P = operating pressure
P_i = partial pressure of species i
P_i^* = equilibrium partial pressure of reactant i
Pr = Prandtl number
r_i = apparent reaction rate between carbon and gas species i
Sc = Schmidt number
T = temperature
T_w = temperature of water in the jacket
v = dimensionless methane composition with respect to molar feed flux of steam
V_c = fraction of space occupied by the unreacted coal particles
w = fraction of remaining carbon in a particle
w_B = fraction of fixed carbon remaining in the ash leaving the gasifier
x = fractional conversion of oxygen
y = fractional conversion of steam
z = height above the grate

Greek Letters

α = radial thermal diffusivity of the bed
γ_i = stoichiometric coefficient of reaction i
ϵ = void volume of the bed
η_i = effectiveness factor for reaction in core
ρ = fractional radius of the unreacted core
ρ_i = density of substance i
ρ_{coal}, ρ_{ash} = densities of original coal and ash segregated from coal particle
λ = system constant determining ratio of carbon monoxide to carbon dioxide as the primary combustion products
θ_c = void fraction in the core of a particle
θ_s = void fraction in the shell of a particle
τ = residence time of coal in the gasifier

LITERATURE CITED

Anthony, D. B., and J. B. Howard, "Coal Devolatilization and Hydrogasification," *AIChE J.*, **22**, 625 (1976).

Argo, W. B., and J. M. Smith, "Heat Transfer in Packed Beds," *Chem. Eng. Progr.*, **49**, 443 (1953).
Aris, R., and N. R. Amundson, *Mathematical Methods in Chemical Engineering*, Vol. 2, pp. 316-328, Prentice-Hall, Englewood Cliffs, N.J. (1973).
Arthur, J. R., "Reactions Between Carbon and Oxygen," *Trans. Faraday Soc.*, **47**, 164 (1951).
Berkowitz, N., "On the Differential Thermal Analysis of Coal," *Fuel*, **36**, 355 (1957).
Carslaw, H. S., and J. C. Jaeger, *Conduction of Heat in Solids*, p. 61, Oxford Press, England (1959).
Chen, J. C., and S. W. Churchill, "Radiant Heat Transfer in Packed Beds," *AIChE J.*, **9**, 35 (1963).
Edgar, T. F., J. M. Galland, B. Dinsmoor, and T. Tsang, "Analysis and Modeling of Underground Coal Gasification Systems," paper presented at AIChE meeting, Chicago, Ill. (Nov., 1976).
Elgin, D. C., and Perks, H. R., "Results of Trials of American Coals in Lurgi Pressure-Gasification Plant at Westfield, Scotland," Sixth Synth. Pipeline Gas Symp., 247 (1974).
Ellman, R. C., and B. C. Johnson, "Slagging Fixed-Bed Gasification at the Grand Forks Energy Research Center," paper presented at the Eighth Synth. Pipeline Gas Symp., Chicago, Ill. (Oct. 18-20, 1976).
———, H. H. Schobert, L. E. Paulson, and M. M. Fegley, "Current Status of Studies in Slagging Fixed Bed Gasification at the Grand Forks Energy Research Center," paper presented at the 1977 Lignite Symposium, Grand Forks, N.D. (May, 1977).
Ergun, S., and M. Menster, "Reactions of Carbon with Carbondioxide and Steam," *Chem. Phys. Carbon*, **1**, 203 (1965).
Feldman, H. F., "The Role of Chemical Reaction Engineering in Coal Gasification," *Advan. Chem. Ser.*, **148**, 132 (1975).
Friedman, L. D., E. Rau, and R. T. Eddinger, "Maximizing Tar Yields in Transport Reactor," *Fuel*, **47**, 194 (1968).
Gaines, A. F., and R. G. Partington, "Differential Thermal Analysis of Mixture of a Low Rank Coal and Various Inorganic Compounds," *ibid.*, **39**, 193 (1960).
Gibson, M. A., and C. A. Euker, Jr., "Mathematical Modeling of Fluidized Bed Coal Gasification," paper presented at AIChE meeting, Los Angeles, Calif. (Nov., 1975).
Gumz, W., *Gas Producers and Blast Furnaces*, Wiley, New York (1950).
Gupta, A. S., and G. Thodos, "Direct Analogy Between Mass and Heat Transfer to Beds of Spheres," *AIChE J.*, **9**, 751 (1963).
Hamm, J. R., "Evaluation of Steag Plant with Coal Gasification at Lünen," *Research Rept. 73-8X1-PDUSY-R1* (Dec., 1973).
Hebden, D., "High Pressure Gasification Under Slagging Conditions," paper presented at Seventh Synthetic Pipeline Gas Symposium, Chicago, Ill. (Oct., 1975).
———, J. A. Lacey, and A. G. Horsler, "Further Experiments With a Slagging Pressure Gasifier," Gas Council Research Communication GC 112 (Nov., 1964).
Hoogendorn, J. C., "Gas From Coal With Lurgi Gasification at Sasol," IGT Symposium Papers, "Clean Fuels from Coal," p. 111 (1973).
Hottel, H. C., and J. B. Howard, *New Energy Technology*, pp. 103-105, MIT Press, Cambridge, Mass. (1971).
Hougen, O. A., K. M. Watson, and R. A. Ragatz, *Chemical Process Principle*, Wiley, New York (1954).
IGT, "Presentation of a Coal Conversion System Technical Data Book," Project 8964, Final Report by IGT for ERDA (Apr., 1976).
Jensen, G. A., "The Kinetics of Gasification of Carbon Contained in Coal Minerals at Atmospheric Pressure," *Ind. Eng. Chem. Process Design Develop.*, **14**, 308 (1975).
Johnson, B. C., H. H. Schobert, and M. M. Fegley, "The Grand Forks Slagging Reactor: Gas-Solid Reactions in the Real World," paper presented at AIChE 70th annual meeting, New York (Nov., 1977).
Jünten, H., and K. H. Van Heek, "Gas Release From Coal as a Function of the Rate of Heating," *Fuel*, **47**, 103 (1968).
Kelly, B. T., and R. Taylor, "The Thermal Properties of Graphite," *Chem. Phys. Carbon*, **10**, 1 (1973).
Kimmel, S., E. W. Neben, and E. E. Pack, "Economics of Current and Advanced Gasification Processes for Fuel Gas Production," *EPRI AF-244*, Project 239, Final Report (1976).
Klose, E., and W. Toufar, "Mathematische Modellierung der Festbett-Druckvergasung," *Energietechnik*, **26**, 546 (1976).
Krieb, K. H., "Combined Gas- and Steam-Turbine Process With Lurgi Coal Pressure Gasification," IGT Symposium papers, "Clean Fuels from Coal," p. 127 (Sept., 1973).
Kunii, D., and O. Levenspiel, *Fluidization Engineering*, Wiley, pp. 61-69, New York (1969).
Lacey, J. A., "Gasification of Coal in a Slagging Pressure Gasifier," *Advan. Chem.*, **69**, 31 (1967).
Lavrov, N. V., V. V. Korobov, and V. I. Filippova, *The Thermodynamics of Gasification and Gas-Synthesis Reactions*, Pergamon Press, Macmillan Co., New York (1963).
Levenspiel, O., *Chemical Reaction Engineering*, 2 ed., pp. 290-293, Wiley, New York (1972).
Loison, R., and F. Chauvin, "Pyrolyse Rapide du Charbon," *Chem. Ind. (Paris)*, **91**, 269 (1964).
Long, S. J., and K. W. Sykes, "The Mechanism of the Steam-Carbon Reaction," *Proc. Royal Soc. (London)*, **A193**, 377 (1948).
Lowry, H. H., *Chemistry of Coal Utilization*, Supplementary volume, p. 913, Wiley, New York (1963).
McIntosh, M. J., "Mathematical Model of Drying in a Brown Coal Mill System. 1.Formulation of Model," *Fuel*, **55**, 47 (1976).
Moe, J. M., "SNG from Coal via the Lurgi Gasification Process," IGT Symposium papers, "Clean Fuels from Coal," p. 91 (Sept., 1973).
Papic, M. M., "Technology and Economics of Coal Gasification," *Can. J. Chem. Eng.*, **54**, 413 (1976).
Parent, J. D., and S. Katz, "Equilibrium Compositions and Enthalpy Changes for the Reactions of Carbon, Oxygen and Steam," *IGT Research Bulletin*, **2** (Jan., 1948).
Phillips, R., F. J. Vastola, and P. L. Walker, "Factors Affecting the Product Ratio of the Carbon-Oxygen Reaction. I and II," *Carbon*, **7**, 479 (1969); **8**, 205 (1970).
Ricketts, T. S., "The Operation of the Westfield Lurgi Plant and the High-Pressure Grid System," paper presented at the 100th Annual General Meeting of the Institution of Gas Engineers, London, England (May, 1963).
Rossberg, M. Z., "Experimentelle Ergebnisse über die Primärreaktionen beider Kohlenstoffverbrennung," *Elektrochem.*, **60**, 952 (1956).
Rudolph, P., "The Lurgi Process, The Route to S.N.G. from Coal," Proc. Fourth Symposium Synthetic Pipeline Gas, Chicago, Ill. (1972).
Sergent, G. D., and I. W. Smith, "Combustion Rate of Bituminous Coal Char in the Temperature Range 800 to 1700°K," *Fuel*, **52**, 52 (1973).
Van Krevelen, D. W., *Coal*, Elsevier Publishing Co., Amsterdam (1961).
Walker, P. L., Jr., F. Rusinko, Jr., and L. G. Austin, "Gas Reactions of Carbon," *Advan. Catalysis*, **2**, 134 (1959).
Walker, W. H., W. K. Lewis, W. H. McAdams, and E. R. Gilliland, *Principles of Chemical Engineering*, McGraw-Hill, New York (1937).
Wen, C. Y., "Optimization of Coal Gasification Processes," R and D Report No. 66, Interim Report No. 1, Office of Coal Research, P N-78 (1972).
———, O. C. Abraham, and A. T. Talwalkar, "A Kinetic Study of the Reaction of Coal Char with Hydrogen-Steam Mixtures," *Advan. Chem. Series*, **69**, 253 (1967).
Wiser, W. H., "A Kinetic Comparison of Coal Pyrolysis and Coal Dissolution," *Fuel*, **47**, 475 (1968).
Woodmansee, D. E., "Modeling of Fixed Bed Gas Producer Performance," *Energy Communications*, **2**, 13 (1976).
———, and J. K. Floess, "Coal Gasifiability Evaluations in a One-Foot Diameter, Fixed-Bed Gas Producer," paper presented at AIChE National Meeting, Houston, Tex. (Mar., 1975).
Woodmansee, D. E., and P. M. Palmer, "Gasification of Highly Caking Coal in the GEGAS Pressurized Gas Producer," paper presented at ACS meeting, New Orleans, La. (1977); preprinted by the Fuels Division.
Yagi, S., and D. Kunii, "Studies on Effective Thermal Conductivities in Packed Beds," *AIChE J.*, **3**, 373 (1957).

Manuscript received July 7, 1977; revision received March 14, and accepted April 24, 1978.